UNIVERSITÀ
DEGLI STUDI
DI PADOVA

Sede Amministrativa: Università degli Studi di Padova

Dipartimento di Istologia, Microbiologia e Biotecnologie Mediche
Sezione di Istologia ed Embriologia

SCUOLA DI DOTTORATO DI RICERCA IN BIOMEDICINA
CICLO XXIV

Role of YAP/TAZ in Mechanotransduction

Direttore della Scuola : Ch.mo Prof. Giorgio Palù

Supervisore : Ch.mo Prof. Stefano Piccolo

Dottorando : Dott.ssa Mariaceleste Aragona

INDEX

ABSTRACT (ENGLISH)

Cells perceive their microenvironment not only through soluble signals but also in term of physical and mechanical cues, such as extracellular matrix (ECM) stiffness or confined adhesiveness. By mechanotransduction systems, cells translate these stimuli into biochemical signals controlling multiple aspects of cell behavior, including growth, differentiation and cancer malignant progression; but how rigidity mechanosensing is ultimately linked to activity of nuclear transcription factors remains poorly understood. Here we report the identification of the *Yorkie*-homologues YAP and TAZ as nuclear relays of mechanical signals exerted by ECM rigidity and cell-shape. This regulation requires Rho activity and tension of the acto-myosin cytoskeleton but is independent from the Hippo/LATS cascade. Crucially, YAP/TAZ are functionally required for differentiation of mesenchymal stem cells induced by ECM stiffness and for survival of endothelial cells regulated by cell geometry; conversely, expression of activated YAP overrules physical constraints in dictating cell behavior. These findings identify YAP/TAZ as sensors and mediators of mechanical cues instructed by the cellular microenvironment.

ABSTRACT (ITALIAN)

Le cellule percepiscono il loro microambiente non solo attraverso molecole segnale e fattori solubili ma anche attraverso stimoli fisici e meccanici. Le cellule traducono questi stimoli in segnali biochimici attraverso un processo definito *meccanotrasduzione*, in grado di regolare numerosi aspetti del comportamento cellulare, tra cui crescita, differenziamento e progressione tumorale. Tuttavia, non è ancora noto come la percezione dei segnali meccanici si traduca nell'attivazione di specifici fattori di trascrizione a livello nucleare. Questo lavoro individua YAP (Yes-associated protein), e TAZ (transcriptional coactivator with PDZ-binding motif, anche noto come WWTR1), omologhi di Yorkie in *Drosophila*, quali fattori di trascrizione in grado di rispondere ai segnali meccanici generati dalla rigidità della matrice extracellulare e dalla forma propria di ogni singola cellula. Questa regolazione richiede l'attivazione della GTPase Rho e la presenza di un citoscheletro di actina contrattile, ma è indipendente dall'attività della via di segnale delle chinasi Hippo e LATS. Non solo YAP/TAZ vengono regolati da segnali meccanici, ma sono anche funzionalmente richiesti per il differenziamento delle cellule staminali mesenchimali indotto dalla *stiffness* (elasticità o rigidità) della matrice e per la sopravvivenza delle cellule endoteliali regolata dalla geometria cellulare. In maniera complementare, l'espressione di una forma attivata di YAP domina sull'azione degli stimoli fisici nel determinare il destino cellulare. Queste scoperte identificano YAP/TAZ come sensori e mediatori degli stimoli meccanici indotti dal microambinete cellulare.

PUBLICATIONS

Leonardo Morsut, Kai-Ping Yan, Elena Enzo, Mariaceleste Aragona, Sandra Maria Soligo, Olivia Wendling, Manuel Mark, Konstantin Khetchoumian, Giorgio Bressan, Pierre Chambon, Sirio Dupont, Regine Losson, Stefano Piccolo. **Negative control of Smad activity by ectodermin/Tif1γ patterns the mammalian embryo.** *Development* 2010 vol .137 (15), pp. 2571-2578.

Sirio Dupont, Leonardo Morsut, Mariaceleste Aragona, Elena Enzo, Stefano Giulitti, Michelangelo Cordenonsi, Francesca Zanconato, Jimmy Le Digabel, Mattia Forcato, Silvio Bicciato, Nicola Elvassore, Stefano Piccolo. **Role of YAP/TAZ in mechanotransduction.** *Nature* 2011 vol. 474 (7350), pp. 179-183.

This work was realized under the mentorship of Dr. Sirio Dupont, and is a consequence of his original ideas, scientific guidance and key experimental contributions .

INTRODUCTION

Physical forces play important roles in living organisms

It is well established that cells can receive information from their surroundings through chemical signals, such as chemokines, hormones and secreted signalling proteins. However, multiple evidence indicate that cells are also able to recognize the physical properties of their microenvironment, ranging from the elasticity of the extracellular matrix to the presence of shear, compressive and stretching forces. Mechanical forces are invariably present within tissues: during early embryonic development, morphogenetic movements at gastrulation are key to place the differentiating tissues in their correct spatial organization; during organogenesis, the forces exerted by blood flow in the vascular system are required not only for the correct branching and patterning of the vascular tree, but also for the establishment of hematopoietic stem cells; in adult life, several tissues such as bone, muscle, and skin constantly remodel themselves in response to external forces (Mammoto and Ingberg 2010). Importantly, mechanical forces are not only required to shape tissues and organs, but are true signals that can deeply influence cell behavior. Indeed, perturbation of the physical and mechanical properties of tissues are often causal to several pathological conditions, contributes to ageing and also plays a role in cancer malignant progression (Jaalouk and Lammerding 2009).

Cells are able to sense the mechanical and physical properties of their microenvironment

The term Mechanotransduction describes the cellular and biochemical mechanisms that translate extracellular mechanical and physical stimuli into intracellular biochemical signals, thus enabling cells to adapt to their physical surroundings. Mechanotranduction implies the following steps (Vogel and Sheetz, 2006):

Mechanosensing

Transmitted forces at some point must impinge on mechanosensitive macromolecules to alter their conformation and hence their function; any changes in normal intracellular force transmission through changes in cellular (or extracellular) structure and organization can lead to altered molecular forces acting on these protein, resulting in attenuated or increased mechanosensitive signals (Fig. 1A). Forces promote changes in protein conformation that accommodate the applied force. The best studied examples are stretch-activated ion channels (Lansman et al., 1987) and receptors (Arnadottir and Chalfie, 2010). At the cell membrane, the integrin layer is oriented with the head domains connecting to the ECM and the cytoplasmic tails binding to focal adhesion kinase (FAK) and paxillin assembled with a stratum containing talin and vinculin, and an uppermost actin-regulatory sheet consisting of zyxin, VASP (vasodilator stimulating phosphoprotein) and alfa-actinin which tethers the FA to the actomyosin cytoskeleton (Kanchanawong et al., 2010). Unfolded protein domains under tension can mediate responses to applied forces. For exemple talin-1, which connects integrins to F-actin, binds to vinculin, which

also links to F-actin, in response to applied forces that unfolds talin-1 exposing the vinculin-binding sites (Ziegler et al. 2008). The adaptor protein p130Cas binds several guanine-nucleotide exchange factors (GEFs) that activate small GTPases, only when phoshorylated by Src family kinases due to cells stretching (Sawada et al., 2006). Integrin receptor itself switches to a high-affinity state in response to force, at least for the ubiquitous $alpha_5beta_1$ isoform (Friedland et al., 2009). In endothelial cells, the glycocalix, a layer of carbohydrate-rich proteins on the cell surface, can mediate mechanotransduction signalling in response to fluid shear stress (Tarbell and Ebong, 2008). Thus, multiple proteins within cells can potentially act as mechanosensors depending on the type of force applied.

Mechanotransmission

In the cytoplasm, the cytoskeleton is the fundamental structure for mediating force transmission. The cytoskeleton is a highly dynamic cellular scaffolding structure composed of filamentous actin, intermediate filaments, and microtubules. Among these elements, the actin cytoskeleton is thought to play a prominent role in force tramsission. Actin monomers assemble into filamentous actin (F-actin) and toghether with myosin filaments, form the cytoskeletal contractile apparatus. The actomyosin cytoskeleton connects multiple parts of the cell membrane as well as the cell membrane to the nucleus. At the cell membrane, these filaments anchor into clusters of proteins that include focal ashesions (FAs) which link the cytoskeleton through transmembrane integrin receptors with the ECM. In the extracellular space, the ECM forms a mesh of crosslinked proteins and carbohydrates, and depending on

the tissue, can include different constituents including collagen, laminin, elastin, and fibronectin fibers interlocked with hyaluronic acid and proteoglycans. Applying force to this cell-ECM unit leads to structural deformations and rearrangements of the ECM, force transmission through the FAs and (given the highly interconnected nature of the cytoskeleton) deformation of nearly each aspect of intracellular structure (Fig. 1A). Adhesion of cells to matrix results in the structural organization of the cell itself. Integrin binding and clustering against ECM ligands leads to changes in cell shape and cytoskeletal architecture, anchoring the actin cytoskeleton to sites of adhesion.

However, "outside-in" force transmission is only half the story, as cells also generate forces: this "inside-out" signaling happens when cells actively pull on the ECM (that in turn responds by remodeling its own 3D organization), as in the case of fibroblasts cotracting a collagen gel. Clearly, cells always generate forces when subjected to external forces in order to develop opposite internal forces to reach an equilibrium. Thus, the ability of cells to develop internal actomyosin forces is likely an inbuilt mechanism by which cells can adjust and perhaps "measure" external forces (Eyckmans et al., 2011). In other words, the tension existing between cells and their ECM always tends to be at equilibrium through reciprocal and self-adjusting outside-in and inside-out signaling.

Mechanoresponse

Cells change their own shape and their cytoskeletal organization in response to mechanical cues (Hoffman et al., 2011). Differences in the substrate avaliable area

or ECM stiffness are tranduced by changes in contractility. Cells plated on soft materials, or cells displaying a rounded or cells with a little adhesion area at their disposal, all exert lower forces than cells on stiff materials or having a spread shape. As a consequence, all the changes in the mechanical properties of the microenvironment ultimately impinge on the ability of the cells to create a tensed actomyosin cytoskeleton (Fig. 1B).

Clearly, the aspect we know the less – and the focus of this thesis – is how cells respond to mechanical signals changing their cell behavior and modulating their gene expression. The following chapter offers some references with some vivid examples of this sort.

How to study Mechanotransduction and role of mechanical cues in Stem Cell differentiation

*Changing cell shape using microfabricated ECM islands .*The first demonstration that physical parameters might be critical for control of cell behavior came almost 30 years ago when it was shown that the growth of anchorage-dependent cells can be altered by changing cell shape, with spread or flattened cells growing more rapidily that round cells (Folkman and Moscona, 1978). Culture of individual cells on microfabricated ECM islands that are small enough to constrain their spreading confirmed that distortion of cell shape and cytoskeletal structure is alone sufficient to govern whether cells will grow, differentiate, or undergo apoptosis (Mammoto and Ingber, 2009). For example, capillary enothelial cells switch from a fate of survival when pleated on large adhesive fibronectin micropatterned to a fate of

death when pleated on small fibronectin micropatterned area (Chen et al., 1997). Similarly, keratinocytes switch between proliferation an differentiation depending on their cell shape (Watt et al., 1998).

Hydrogels. More recently, developing scaffolds with tunable mechanical properties, mimicking the natural variation of microenvironment rigidity, has become a major effort in tissue engineering (Choi et al, 2010). Real tissues are indeed endowed with a whide range of stiffness (Fig. 2A); the brain, for instance, is much softer than bone tissue. The rigidity of the extracellular environment potently controls the differentiation of mesenchymal stem cell (MSC), as well as the balance between proliferation and self renewal in skeletal muscle stem cell (Engler et al., 2006) (Gilbert et al., 2010), hematopoietic stem cells (Holst et al, 2010) and embryonic stem cells (Chowdhury et al., 2010). Depending on the soluble factors in medium, MSCs will adopt the adipogenic (McBeath et al., 2004; Sordella et al., 2003) or condrogenic (Gao et al., 2010) phenotype when cell size is restricted or when contractility is reduced. Conversely, spreading and high contractility promotes osteogenic (McBeath et al., 2004) and myogenic differentiation (Gao et al., 2010). Stiffness also dictates differentiation of MSCs (Fig. 2B) towards a neurogenic or adipogenic phenotype on compliant substrates (<1 kPa), myogenesis at medium stiffness (8-17 kPa), and osteogenesis at high stiffness (>25 kPa) (Engler et al., 2006; Fu et al., 2010).

Mechanotransduction in pathology

Tissue rigidity or stiffness and also the mechanotransduction machinery affects many pathological proceses. Tumours have long been identified by palpation, owing to local increases in tissue stiffness. Concurrent changes in tissue stiffness, tumor growth due to the proliferting cells and elevated interstitial fluid pressure all combine to affect the physical environment of cancerous cells inside the tumor and the adjacent normal cells (Butcher et al., 2009). These changes in the mechanical environment have been shown to be causal of tumor progression in breast (Levental et al., 2009): induction of collagen crosslinking stiffened the ECM, promote focal adhesion and induce the invasion of an oncogene-inititated epithelium. Fibrotic lung disease begins with a small change in tissue stiffness, inducing more severe, irreversible remodelling with a feedback relationship between matrix stiffening, cyclooxygenese-2 (COX-2) suppression and fibroblast activation that promotes and amplifies progressive fibrosis (Liu et al., 2010). Disturbed fluid shear stress at vascular bifurcations, that trigger vessel remodelling, can result in development of atherosclerosis (Hahn and Schwartz, 2009). Many mutations in structural cardiac mechanotransducres proteins can result in cardiomyopathy and pathological hypertrophy (reviewed in Jaalouk and Lammerding, 2009). In Duchenne muscular dystrophy, mutations in the dystrophin gene disrupt the force transmission between the cytoskeleton and the ECM, resulting in progressive muscle degeneration (Kumar et al., 2004). Mutations in the cytoskeletal proteins desmin, titin and myosin, result in disorganized sarcomeres and disturbed cellular mechanics, which can impair relaxation dynamics of myocytes. Mutations in the

genes that encode the ciliary proteins polycystin 1 or the transient receptor potential channel family protein polycystin 2 (TRPP2), that act as cellular flow-sensors, provide direct evidence for defects in mechanotransduction that result in kidney disease (Delmas, 2004). In general, all aspects of mechanoperception can affects pathological conditions.

Signalling pathways involved in Mechanotransduction

Application of tension to cells activate different signalling pathways by which cells communicate the dynamic status of their actin microfilaments to the genome.

Mechanical stimuli activate different members of the Rho GTPase (Rho, Rac and Cdc42 subfamilies) which regulate effector proteins that modulate the polymerization equilibrium of G-actin and F-actin in the cytoplasm. G-actin forms complexes with different actin binding proteins (ABPs), including the nucleating factors profilin, formins and the actin-related protein 2/3 (ARP2/3) complex (reviewed in Olson and Nordheim, 2010). Activation of Rho GTPase promotes actin polymerization by two downstream signalling modules, one involving the Rho-associated kinase (ROCK) and the other mediated by formins such as Diaphanous.

Signals that elicit dynamic actin rearrangements on activation of Rho GTPase, where shown to activate the Jun N-terminal kinases (JNKs), which regulate gene transcription (Marinissen et al., 2004); to regulate the cytoplasm to nucleus translocation of the transcription factor Nuclear Factor kB (NF-kB) (Cowell et al., 2009); to signal to phosphoinoside 3-kinase (PI 3-kinase) which activates proliferation through the Akt pathway (reviewed in Provenzano and Keely, 2011);

to modulate TGFb (Moustakas and Heldin, 2008) and Wnt-planar cell polarity (PCP) signalling (Winter et al., 2001). The amount of G-actin control the nucleus-cytoplasm shuttling of transcriptional cofactors of the myocardin related transcription factors (MRTFs, one of wich is MAL) that, in turns, control the activity of serum response factor (SRF), a nuclear transcription factor. High levels of cytoplasmic G-actin retain MAL in the cytoplasm, incorporation of G-actin into the F-actin filament liberates MAL to enter the nucleus and interact with SRF (Vartiainen et al., 2007). Thereby, the actin-MAL-SRF circuit allows for the precise modulation of gene expression in concert with cytoskeletal assembly and disassembly.

Moreover, mechanosensing Fas contain many signaling proteins such as FAK, extracellular signal-regulated kinase (ERK), mitogen-activated protein kinase (MAPK), c-Jun N-terminal kinase (JNK), Src, Ras and Raf; changes to composition of such adhesions mediated by contractility can impact localization of members within a signaling cascade, thereby orchestrating cellular responces to force. Acute onset of shear stress triggers the activation of the transcriptional factor NF-kB (nuclear factor of kappa light chain gene enhancer in B cell) (Tzima et al., 2005) in response to changes in F-actin polymerization and cell stretching (Olson and Nordheim, 2010).

However, despite intense efforts, the involvement of nuclear factors mediating the biological response to ECM elasticity and cell geometry, linking mechanical stimuli with genome activity, remained so far incompletely understood.

The Hippo pathway

The Hippo signaling pathway has emerged as an important regulator in both organ size control and tumorigenesis. First discovered in *Drosophila* (Fig. 3A and 4A), the Hippo pathway is composed of a highly conserved core kinase cascade leading from the tumor suppressor Hippo (Mst1 and Mst2 in mammals) to the oncoprotein Yorkie (YAP and TAZ in mammals), a transcriptional coactivator of target genes involved in cell proliferation and survival (Pan, 2010). Many of the known Hippo Pathway components were discovered through genetic screens in *Drosophila.* Loss of function of Hippo (Hpo) or Warts (Wts), two kinases that lie at the center of the Hippo pathway, results in dramatic overgrowth of imaginal discs and of corresponding adult structures (Harvey et al., 2003; Jia et al., 2003; Justice et al., 1995; Wu et al., 2003; Xu et al., 1995). Animals with Hpo mutant eye discs, for expemple, produce adults with severely overgrown eyes and heads that are folded and darker than normal (reviewed in Halder and Johnson, 2011). The Hpo gene was thus named after its mutant adult head phenotype, which resembles the hide of the hippopotamus (Udan et al., 2003). The identification of the scaffolding protein Salvador (Sav) (Tapon et al., 2002) and the regulator Mob-as-tumor suppressor (Mats) (Lai et al., 2005) leads to the understanding of the core component of the pathway. These proteins propagate a cascade of phosphorylation events that result in to the inhibition of the trascriptional regulator Yorkie (Yki). Phosphorilated Yki is competent to bind 14-3-3 proteins, which function to retain Yki in the cytoplasm and consequently inhibit Yki nuclear function (reviewed in Mauviel et al., 2011). Overexpression of Yki phenocopies loss of function mutations of Hpo or Wts

including tissue overgrowth in wing imaginal discs (Huang et al., 2005), (Fig. 3B).

The core component of the Hippo pathway is well conserved in mammals: Mst1 and Mst2 are the two homologue of Hpo, Sav1 or WW45 is the homolog of Sav, Lats1 and Lats2 are the homologue of Wts and MOBKL1A and MOBKL1B, often collectively referred as Mob1, are the homologs of Mats. These protein form a conserved kinase cassette (Chan et al., 2005; Callus et al., 2006) that phosphorilates and inhactivates the mammalian Yki homologs YAP (Yes-associated protein) (Dong et al, 2007; Zhao et al., 2007) and TAZ (transcriptional coactivator with PDZ-binding motif, also known as Wwtr1) (Lei et al., 2008). YAP/TAZ localization, and hence activity, directs their interactions with a wide array of proteins, which range from DNA-binding transcription factors to cell-polarity-regulating proteins (Fig. 3A and 4A) and respond to cell contact inhibition, since the subcellular localization of YAP/TAZ is dependent on cell density (Zhao et . al., 2007).

YAP/TAZ localization is largely mediated by interaction with 14-3-3 proteins (Kanai et al, 2000; Basu et al., 2003). These interaction are promoted by LATS1/2 induced phosphorilation of YAP/TAZ (Dong et al., 2007; Lei et al., 2008) on multiple residues: S61, S109, S127, S164, S381 for YAP and S66, S89, S117, S311 for TAZ, wich only one (YAP S127 and TAZ S89, like Yki S168) serves as 14-3-3 binding site. The phospho-degron motif in YAP and TAZ is induced by LATS kinases and further modified by Casein Kinase 1 delta/epsilon kinases resulting in the recruitment of the E3 ubiquitin ligase SCF beta-TRCP and subsequent ubiquitin-mediated proteasomal degradation of YAP and TAZ (Liu et al., 2010; Zhao et al., 2010).

The physiological relevance of the conserved Hippo kinase cascade was

supported by studies of transgenic and knockout mice. Transgenic overexpression of YAP (Fig. 4B) (Dong et al., 2007; Camargo et al, 2007) or liver-specific knockout of Mst1/2 or Sav1 (Zhou et al., 2009; Lee et al., 2010) expanded the liver size and ultimately induced hepatocellular carcinoma (HCC), revealing a conserved role for the Hippo pathway in regulating organ size in mammals. YAP and TAZ function as transcriptional co-activators by means of physical interaction with a range of DNA-binding transcription factors, such as the TEAD/TEF family transcription factors, the p53 family members p73, Runx1 and Runx2, Pax3, Pax8, TTF1,TBX5, PPARgamma (reviwed in Pan, 2010) and SMAD1/2/3/4 (reviewed in Mauviel et al, 2011). Among these YAP/TAZ interactin proteins, the TEAD/TEF family transcription factors, which represent homologs of the *Drosphila* Scalloped (Sd) protein, have emerged as the prime mediators of YAP/TAZ function in Hippo signalling (Zhao et al., 2008; Ota and Sasaki, 2008). Several upstream regulators of the Hippo pathway have been identified in *Drosophila*, all of which, when mutated, result in tissue overgrowth. These include: the FERM domain proteins Merlin (NF2 in mammals) and Expanded; the atypical cadherins Fat and Dachsous whit the regulators Kibra and Zyxin; the transmembrane polarity-regulator Crumbs; the cell polarity factors Lethal giant larvae (Lgl), Discs large (Dlg), Scribble (Scrib); Jub (Ajuba LIM proteins in mammals); the Ras association family protein RASSF (reviewed in Zhao et al., 2011a). Other regulators have been identified only in mammals: the Crumbs complex-associated protein PALS1 (Varelas et al., 2010), Angiomotin (AMOT) (Zhao et al, 2011b), the adherent juction-associated protein alfa-catenina (Schlegelmilch et al., 2011; Silvis et al., 2011) and the tight junction protein ZO-2 (Oka et al., 2010;

Remue et al., 2010).

The critical role in development of the protein YAP is fully highlight by the knockout mice that are embryo lethal (Morin-Kenscki et al., 2006), while TAZ knockout mice develop polycystic kidney disease and emphysema (Hossain et al., 2007; Makita et al., 2008). In the preimplantation mouse embryo YAP is fundamental for the specification of the trophectoderm from the inner cell mass (Nishioka et al., 2009): YAP localizes at the nuclei of outside cells promoting TEAD4 activity, while YAP is phosphorilated and cytoplasmic in inside cells.

YAP/TAZ and Stem Cells

Emerging evidences suggests that YAP and TAZ may regulate stem cell and progenitor cell self-renewal and expansion. For instance, YAP expression is generally restricted to the progenitor cells in normal mouse intestine, and transgenic expression of YAP in mouse intestines causes a marked expansion of the progenitor cell compartment (Camargo et al., 2007). Similarly, YAP expression expands basal epidermal progenitors in mouse skin and inhibits their terminal differentiation (Zhang et al., 2011), while conditional knockout of YAP in mouse skin leads to decrease proliferazion of basal cells, thinner epidermis and failure of skin expansion (Schlegelmich et al., 2011). These observation reflect a role of YAP in maintaining the balance between stem, progenitor and differentiated cells.

Morover, the YAP/TAZ-TEAD transcription factor complex represents a common target of oncogenic transformation. Amplification of the *YAP* and *TAZ* gene loci have been reported at varying frequencies in a wide spectrum of human tumors.

Consistently, comprehensive survey of the most common solid cancer types revealed widespread and frequent YAP and TAZ overexpression (Pan et al., 2010).

Malignant progression is accompanied by increase proportion of these CSCs within the tumor (Pece et al., 2010) and activation of the epithelial-to-mesenchymal transition (EMT) trigger by loss of cell polarity (Thiery et al., 2009). In our laboratoriy, it was shown that TAZ is a molecular determinant of biological properties associated with breast Cancer Stem Cells (CSCs), namely self-renewal and tumor-initiation capacity. TAZ sustained CSCs maintenance downstream of EMT and delocalization of the basolateral protein Scribble (Cordenonsi et al., 2011).

In summary, YAP and TAZ are required for many physiological and pathological processes including contact inhibition, epithelial-mesenchimal transition, transformation, apoptosis inhibitions and cell differentiation.

RESULTS

ECM stiffness regulates YAP/TAZ activity

Mechanotransduction enables cells to sense and adapt to external forces and physical constraints; these mechanoresponses involve the rapid remodeling of the cytoskeleton, but also require the activation of specific genetic programs.

To gain insight into these issues, we asked if physical/mechanical stimuli conveyed by ECM stiffness actually signal through known signaling pathways. For this, we performed a bioinformatic analysis on genes differentially expressed in mammary epithelial cells (MEC) cultivated on ECM of high vs. low stiffness (Provenzano et al., 2009). Specifically, we searched for statistical associations between genes regulated by stiffness and gene signatures denoting the activation of specific signaling pathways such as TGF-beta, Ras, ErBB2, Notch, Wnt/b-catenin, MAL/SRF and NF-kB (see Methods). Strikingly, only signatures revealing activation of YAP/TAZ transcriptional regulators emerged as significantly overrepresented in the set of genes regulated by high stiffness (Fig. 5A).

To test if YAP and TAZ activity is regulated by ECM stiffness, we monitored YAP/TAZ transcriptional activity in human MEC cultured on fibronectin-coated acrylamide hydrogels of varying stiffness (elastic modulus ranging from 0.7 to 40 KPa, matching the physiological elasticities of natural tissues (Engler et al., 2006)). For this, we assayed by real-time PCR two of the best YAP/TAZ regulated genes from our signature, *CTGF* and *ANKRD1.* The activity of YAP/TAZ in cells cultured on

stiff hydrogels (15-40 KPa) was comparable to that of cells grown on plastics, whereas culturing cells on soft matrices (in the range of 0.7-1 KPa) inhibited YAP/TAZ activity, to levels comparable to siRNA-mediated YAP/TAZ depletion (Fig. 5B). We confirmed this finding in another cellular systems, such as MDA-MB-231, where we used a synthetic YAP/TAZ-responsive luciferase reporter (4xGTIIC-lux) as direct read-out of their activity (Fig. 5B).

Next, we assayed endogenous YAP/TAZ subcellular localization; indeed, their cytoplasmic relocalization has been extensively used as primary read-out of their inhibition by the Hippo pathway or by cell-cell contact (Zhao et al., 2007). By immunofluorescence on MEC and human mesenchymal stem cells (hMSC), YAP/TAZ were clearly nuclear on hard substrates but became predominantly cytoplasmic on softer substrates (Fig. 5C and 5D). Collectively, these data indicate that YAP/TAZ activity and subcellular localization are regulated by ECM stiffness.

YAP/TAZ are regulated by cell geometry

As changes in ECM stiffness impose different cell shapes (Engler et a., 2006), we thus asked whether cell spreading is sufficient to regulate YAP/TAZ. To this end, we used micropatterned fibronectin "islands" of defined size, on which cells can spread to different degrees depending on the available adhesive area (Chen et al., 1997). On the biggest islands (10000mm^2) hMSC cells covered almost the entire area, adopting a similar shape to cells plated on unlimited surfaces; by progressively limiting the adhesion areas (2025, 1024, 300mm^2), cells assumed the shape of the supporting island and started to become more rounded. On these micropatterns, the

localization of YAP/TAZ changed from predominantly nuclear in spread cells, to predominantly cytoplasmic in cells on smaller islands (Fig. 6A). Of note, the use of single-cell adhesive islands rules out the possibility that cell-cell contacts could be involved in YAP/TAZ relocalization. We confirmed these results using human lung microvascular endothelial cells (Fig. 6B), that are well known to regulate their growth according to cell shape (Chen et al., 1997).

Cells seeded on stiff hydrogels or large islands display an increased cell spreading but, at the same time, experience a broader cell-ECM contact area. To test if YAP/TAZ are regulated by cell spreading irrespectively of the total amount of ECM, we visualized YAP/TAZ localization in hMSC grown on the tip of closely arrayed fibronectin-coated micropillars (Fu et al., 2010): on these arrays, cells stretch from one micropillar to another, and assume a projected cell area comparable to cells plated on big islands (3200 mm^2 on average, Fig. 6C); however, in these conditions, the actual area available for cell/ECM interaction is only about 10% of their projected area (300 mm^2 on average, corresponding to the smallest islands used in Fig. 6A). YAP/TAZ remained nuclear on micropillars (Fig. 6C, indicating that YAP/TAZ are primarily regulated by cell spreading imposed by the ECM.

YAP/TAZ sense cytoskeletal tension

We then considered that cell spreading entails activation of the small GTPase Rho that, in turn, regulates the formation of actin bundles, stress fibers and tensile actomyosin structures (Schwartz, 2010). Indeed, cells on stiff ECM or big islands

displayed more prominent stress fibers compared to those plated on soft ECM or small islands (Fig. 6B and 6D). As shown in Figure 7A, we found that Rho and the actin cytoskeleton are required to maintain nuclear YAP/TAZ. As a control, inhibition of Rac1-GEFs, or disruption of microtubules, did not alter YAP/TAZ localization (Fig. 7A). Crucially, inhibition of Rho (with the cell permeable C3 transferase) and of the actin cytoskeleton (with LatrunculinA) also inhibited YAP/TAZ transcriptional activity, as assayed by expression of endogenous target genes (Fig. 7B) and by luciferase reporter assays (Fig. 7C). Conversely, triggering F-actin polymerization and stress fibers formation by overexpression of activated Diaphanous promoted YAP/TAZ activity (Fig. 7D).

We then asked whether YAP/TAZ are regulated by the ratio of monomeric/filamentous actin, as others observed for MAL/SRF. To increase monomeric G-actin, we overexpressed the R62D mutant actin (Miralles et al., 2003), but this was insufficient to inhibit YAP/TAZ (Fig. 7C). Moreover, increasing the amount of F-actin either by overexpressing the F-actin stabilizing V159N actin mutant or by serum stimulation (Miralles et al., 2003) had no effect on YAP/TAZ activity (Fig. 7E). As a control, in the same experimental set-up, MAL/SRF activity was instead clearly modulated (Fig. 7F). Taken altogether, these data indicate that Rho and stress fibers, but not F-actin polymerization *per se*, are required for YAP/TAZ activity.

Cells respond to the rigidity of the ECM by adjusting the tension and organization of their stress fibers, such that cell spreading is accompanied by increased pulling forces against the ECM (Fu et al, 2010; Schwartz et al., 2010). By

inhibition of ROCK (with the Y27632 small molecule inhibitor) and non-muscle myosin (NMM-II, with Blebbistatin) (Engler et al., 2006; Vogel and Scheetz, 2006), we found that cytoskeletal tension is required for YAP/TAZ nuclear localization (Fig. 8A) and activity (Fig. 8B). Of note, YAP/TAZ exclusion caused by these inhibitions is an early event (occurring within 2 hours) that can be uncoupled from destabilization of stress fibers (Fig. 8C). To address more directly the relevance of cell-generated mechanical force without using small-molecule inhibitors and irrespectively of the surface properties of the hydrogels, we compared rigid vs highly elastic micropillars (Fu et al., 2010); on the elastic substrate, cytoplasmic localization of YAP/TAZ was clearly increased (Fig. 8D). Collectively, the data indicate that YAP/TAZ respond to cytoskeletal tension.

We also tested if inhibition of YAP/TAZ occurs by entrapping YAP/TAZ in the cytoplasm or by promoting their nuclear exclusion. In *Drosophila,* the YAP/TAZ homologue Yorkie is exported from the nucleus in a CRM1-dependent manner (Ren et al, 2010); this regulation allowed us to test if YAP/TAZ nuclear exit triggered by cytoskeletal inhibitors could be reverted by the addition of the CRM1 inhibitor LeptomycinB (LMB). As shown in Figure 9A, LMB rescued nuclear localization of YAP/TAZ in hMSC treated with cytoskeletal inhibitors. These data suggest that YAP/TAZ keeps shuttling between cytoplasm and nucleus irrespectively of cell shape, and that the presence of a stretched cytoskeleton promotes their nuclear retention. Moreover, YAP/TAZ relocalization was rapid (occurring in as little as 30 min with LatrunculinA), reversible after small-molecule washout (Fig. 9B), and insensitive to inhibition of protein synthesis with Cycloheximide (CHX) (Fig. 9C),

suggesting a direct biochemical mechanism.

Mechanical cues act independently from Hippo

YAP and TAZ are the nuclear transducers of the Hippo pathway. In several organisms and cellular set-ups, activation of the Hippo pathway leads to YAP/TAZ phosphorylation on specific serine residues; in turn, these phosphorylations inhibit YAP/TAZ activity through multiple mechanisms, including proteasomal degradation (Pan et al., 2010). Intriguingly, similar to Hippo activation by cell-cell contacts (Fig. 10A), TAZ protein was also degraded by culturing MEC cells on soft matrices (Fig. 10B) or by treatment with inhibitors of Rho, F-actin and actomyosin tension (Fig. 10C).

Is then the Hippo cascade responsible for YAP/TAZ inhibition by mechanical cues? Several evidences indicate this is not the case. First, we noted that phosphorylation of YAP on serine 127, a key target of the LATS kinase downstream of the Hippo pathway (Oka et al., 2008), was not increased upon treatment of hMEC and hMSC with cytoskeletal inhibitors (Fig. 10B) at difference with its regulation by high confluence (Fig. 10A). Second, depletion of LATS1 and LATS2 had marginal effect on YAP/TAZ inactivation by mechanical cues, as judged by: i) YAP/TAZ nuclear exit induced by micropatterns (Fig. 10C); ii) TAZ degradation (Fig. 10D); iii) endogenous target gene expression in cells plated on soft hydrogels (Fig. 10E). Finally, we compared wild-type or LATS-insensitive 4SA TAZ (Let at al., 2008) in MDA-MB-231 depleted of endogenous YAP/TAZ and reconstituted at near-to-endogenous YAP/TAZ activity levels with siRNA-insensitive mouse TAZ (mTAZ) vectors. As shown in Fig. 10F, both wild-type (WT) and 4SA mTAZ remain sensitive

to mechanical cues. Further supporting these results, we found that MDA-MB-231 cells are homozygous mutant for NF2/merlin, an essential component of the Hippo cascade (Pan et al., 2010). Collectively, these data suggest that LATS phosphorylation downstream of the Hippo cascade is not the primary mediator of mechanical/physical cues in regulating YAP/TAZ activity.

We then asked if mechanical cues regulate YAP/TAZ not only in isolated cells, but also in confluent monolayers, when cells reorganize their shape and structure and engage in cell-cell contacts, leading to activation of Hippo/LATS signaling (Zhao et al., 2007). We explored the effects of cell confluence in parental MCF10A: plating cells at high confluence cooperate with soft hydrogels in inhibiting YAP/TAZ activity (Fig. 10G). Thus, mechanical cues and Hippo signaling represent two parallel inputs converging on YAP/TAZ regulation.

YAP/TAZ mediate cellular mechanoresponses

Data presented so far indicate YAP and TAZ as molecular "readers" of ECM elasticity and cell geometry; but are YAP/TAZ relevant to mediate the biological responses to these mechanical inputs? An appropriate cellular model to address this question are hMSC, that can differentiate into osteoblasts when cultured on stiff ECM, mimicking the natural bone environment, while on soft ECM – or small islands – they differentiate into other lineages, such as adipocytes (McBeath et al., 2004; Engler et a., 2006). A similar case applies to endothelial cells, that respond differently to the same soluble growth factor by proliferating, differentiating or involuting according to the degree of cell spreading against the surrounding ECM (Chen et al., 1997). We

hypothesized that cell fates induced by stiff ECM and large islands (i.e. where YAP/TAZ are active) should require YAP/TAZ function and, conversely, cell fates associated to soft ECM and small islands (where YAP/TAZ are inhibited) should require their inactivation. In line with this hypothesis, osteogenic differentiation induced in hMSC on stiff ECM was inhibited upon depletion of YAP and TAZ, and a similar inhibition was achieved either by culturing cells on soft ECM or by incubation with C3 (Fig. 11A and 11B). We also monitored adipogenic differentiation, a fate normally not allowed on stiff ECM; strikingly, YAP/TAZ knockdown enabled adipogenic differentiation on stiff substrates, thus mimicking a soft environment (Fig. 11C and 11D). In the case of HMVEC, cells plated on small islands undergo apoptosis, while cells on bigger islands proliferate, as assayed by TdT-mediated dUTP nick end labelling (TUNEL) staining and 5-bromodeoxyuridine (BrdU) incorporation, respectively (Chen et al., 1997). Upon YAP/TAZ depletion, cells on bigger islands behaved as if they were on small islands; this is overlapping with the biological effects of Rho inhibition (Fig. 12A and 12B). In line with the Hippo independency of this regulation, knockdown of LATS1/2 was not sufficient to rescue osteogenesis upon C3 treatment (Fig. 13B), or endothelial cell proliferation on small islands (Fig. 12C). Collectively, these data suggest that YAP/TAZ are required for cell differentiation triggered by changes in ECM stiffness and for geometric control of cell survival.

We next tested if the sole YAP/TAZ activity can re-direct the biological responses elicited by soft/confined ECM. Overexpression of activated 5SA-YAP with lentiviral infection (to at least ten fold the endogenous levels) remarkably overruled

the geometric control over proliferation and apoptosis in HMVEC (Fig. 12D), and rescued osteogenic differentiation of hMSC treated with C3 (Fig. 13A) or plated on soft ECM (Fig. 13C). Thus, cells on soft matrices or on small adhesive areas can be "tricked" to behave as if they were adhering on harder/larger substrates by sustaining YAP/TAZ function.

DISCUSSION

In sum, our findings indicate a fundamental role of the transcriptional regulators YAP and TAZ as downstream elements in how cells perceive their physical microenvironment (Fig. 14A). This is linked to the capacity of cells to generate pulling forces against a rigid ECM that favors the adoption of a spread shape. Our data define an unprecedented modality of YAP/TAZ regulation, that acts in parallel to the NF2/Hippo/LATS pathway and instead requires Rho activity and the acto-myosin cytoskeleton.

Comparison with the MAL/SRF system. Interestingly, this recapitulates aspects of MAL/SRF regulation (Miralles et al., 2003; and see introduction of this thesis) because both YAP/TAZ and MAL are inhibited by F-actin disruption and stimulated by F-Actin polymerization. Yet there are profound differences: YAP/TAZ activity requires stress fibers and cytoskeletal tension induced by ECM stiffness and cell spreading, but, at difference with MAL, YAP/TAZ are not directly regulated by G-actin levels. Of note, the role of cell morphology and stress fibers in the regulation of YAP localization is also supported by others (Wada et al., 2011,; Sansores-Garcia et al., 2011). The detailed biochemical mechanisms by which cytoskeletal tension regulates YAP/TAZ awaits further characterization, but it is tempting to speculate that stress-fibers inhibit/titrate an unidentified YAP/TAZ-interacting molecule that, when released, would promote their inactivation ("X" in Fig. 14B).

Lessons from Drosophila. Independent evidence from *Drosophila* embryos also suggests that the actin cytoskeleton is indeed an important regulator of Yorkie (Yki),

the fly homologue of YAP/TAZ, during embryonic development (Garcia-Fernandez et al., 2011; Sansores-Garcia et al., 2011). These groups identified the F-actin capping proteins (CP, also known as beta-actinin or capZ) as required inhibitors of Yki functions. Knockdown of CP or mutant alleles for CP cause increased tissue growth and upregulation of Yki activity in the *Drosophila* wing ephitelium, similar to those obtained in mutants for components of the canonical Hippo cascade, such as Hpo or homologues of the LATS kinases.

New mechanistic hints? An interesting point of discussion is whether these genetic validations in *Drosophila* of the role of cytoskeleton as regulator of Yki/YAP/TAZ may also suggest some mechanistic insights. For example, F-actin might regulate Yki through the Hippo/LATS pathway. The Halder laboratory (Sansores-Garcia et al., 2011) suggested that F-actin acts downstream of the Hippo kinase but upstream of Warts (Wts), the fly omologue of LATS (Sansores-Garcia et al., 2011). However, this interpretation is biased by the fact that in *Drosophila* LATS mutants are by far stronger than Hpo and CP mutants, complicating the interpretation of the genetic interactions. Moreover, Janody group, also working in *Drosophila* (Garcia-Fernandez et al., 2011), reached partially different conclusions, that is, that F-actin capping proteins may work upstream of Hippo kinase. In any case, both studies at least suggest that LATS activity, more or less directly, should increase after cytoskeletal re-organization. Supporting this conclusion, Wada et al., 2011, found that YAP phosphorylation in LATS sites increases after disruption of the actin cytoskeleton using Latrunculin A, the F-actin disgregating factor. Clearly, this body of evidence apparently contrasts with our conclusion that mechanical-induced

cytoskeletal reorganization (MSC plated on soft; endothelial cells plated on small islands) leading to drop of YAP/TAZ activity dominates over and remains insensitive to LATS1/2 depletion. There are several solutions to accomodate these different observations: 1) it is plausible that actin disruption may be profoundly different than a mechanically "soft" stimuli; it should be stressed in this point that even in *Drosophila* it is not F-actin per se to regulate YAP/TAZ. Indeed, there are other mutations in actin inhibitors (i.e., cofilin) that induce F-Actin accumulation without activating YAP/TAZ; 2) finding YAP phosphorylation and LATS activation upon F-actin disruption does not reveal per se functional causality; 3) it is also plausible that LATS activation may well be induced by cytoskeletal re-organization, but that this is only one inhibitory branch activated by the disturbed cytoskeleton, such that loss-of-LATS alone would be insufficient to rescue YAP-TAZ activity (due to the persistence of other, yet unknown unleashed inhibitors that would remain present even in LATS-depleted cells); 4) It is also conceivable that the biological potency of LATS inactivation is directly proportional to the "basal"/"natural" level of Hippo pathway activation in a given cellular context. For example, a cell like MDA-231 lacks of NF2 and is therefore silent for Hippo. Thus, not surprisingly, loss of LATS is completely irrelevant for these cells at regulating YAP/TAZ transcriptional activity. Yet, MDA-231 are perfectly capable of regulating YAP/TAZ when challenged by mechanical cues (data not shown). Conversely, in cells normally carrying a constitutive Hippo pathway, such as MCF-10A cells, loss-of-LATS has more potent pro-YAP effects. And yet, even in this case, this is insufficient to sustain YAP activity in a soft environment, that still leads to a dramatic attenuation of YAP/TAZ activity.

In other words, the collective evidence on one hand does suggest an involvement of LATS in mechanotransduction but on the other hand also strongly indicate that this is only a fragment of a more complex picture that we are struggling to grasp mechanistically. If anything, data indicate that mechanical cues is an universal feature of Yki/YAP/TAZ regulation, and that inputs from the LATS branch may concur in more specific contexts (see the MDA-231 vs MCF10A scenarios). Finally, feedback loops are likely in place, as it has been shown that the Hippo pathway could inhibit F-actin accumulation (causing a coherent crosstalk between two inhibitory branches); and conversely, F-actin was proposed to operate as scaffold for Mst1/2 (Densham et al., 2009), suggesting a possible direct link between F-actin and Hippo proteins.

Placing YAP/TAZ downstream of the cell biology of Mechanotransduction. Functionally, we showed that different cellular models read ECM elasticity, cell shape and cytoskeletal forces as levels of YAP/TAZ activity; but what is more remarkable is that experimental manipulations of YAP/TAZ levels can dictate cell behavior, overruling mechanical inputs. YAP/TAZ are very active and able to bypass the effect of a soft, round and cytoskeletally disorganized cell, to rescue gene expression and differentiation potential normally allowed only at higher mechanical stimulations.

Relevance for diseases and organ remodeling. This work identifies a new widespread transcriptional mechanism by which the mechanical properties of the ECM and cell geometry instruct cell behavior. This may now shed light on how physical forces shape tissue morphogenesis and homeostasis, for example in tissues

undergoing constant remodeling upon variation of their mechanical environmnent; indeed, alterations of YAP/TAZ signaling have been genetically linked in animal models to the emergence of cystic kidney, pulmonary emphysema, heart and vascular defects (Chen et al., 1994; Makita et al., 2008; Morin-Kensicki et al., 2006; Skouloudaki et al., 2009).

Relevance for tumor progression. In cancer, changes in the ECM composition and mechanical properties is the focus of intense interest, as these have been correlated with progression and build-up of the metastatic niche (Jaalouk et al., 2009); in light of their powerful oncogenic activities (Pan, 2010) YAP/TAZ might serve as executers of these malignant programs. This is a particularly exciting possibility, at least in breast cancer: first, tumor progression has been shown to correlate with an increase of cancer stem cells (CSCs) that directly impact on tumor grading (Pece et al., 2010); second, we found that TAZ is playing a causal role in CSCs maintenance and in acquisition of CSCs-phenotypic traits (Cordenonsi et al., 2011). Clearly, closing the link between CSCs, TAZ, and ECM mechanorigidity is the focus of our on-going work.

Mechanical stress, organ size and organ proliferative homeostasis. Genetically, YAP and TAZ have been linked to a universal system that control organ size (Pan, 2010). The current view implicates Hippo signaling as the sole determinant of YAP/TAZ regulation in tissues. However, our results suggest physical/mechanical inputs as alternative determinant of YAP/TAZ activity. Supporting our model, it has been observed that growth of epithelial tissues entails the build-up of mechanical stresses at tissue boundaries (Nienhaus et al., 2009), and theoretical work proposed

that these serve as positive feedback to homogenize cell growth, compensating for uneven activity of soluble growth factors (Schwank and Basler, 2010).

Conclusion. In the last 20 years, progress in understanding signal transduction have permeated biology: we know the main growth factor signaling pathways and have charted networks of protein-protein interactions and gene expression programs that control cell fates during embryonic development, tissue homeostasis and disease. However, a true "holistic" appreciation of the molecular mechanisms governing cell behavior cannot be uncoupled by an equally in depth appreciation of their spatial and temporal control occurring at the tissue level. Although this represents a phenomenally difficult task, there is an increasing appreciation that tissue architecture, as defined by the spatial organization of a cell in respect of its neighbors and the extracellular matrix (ECM), represents in its own right an overarching regulator of cell growth, migration, differentiation and stemness. Key elements of this architectural signal are cell polarity, cell adhesion and the corresponding mechanics of the cytoskeleton. We can only define as remarkable the fact that nuclear YAP/TAZ levels emerged in the last year - and with seminal contribution from our group - as central sensor and mediators of structural and architectural properties of tissues. It should also not go unnoticed that a single set of transcriptional regulators is at the center of some "classic" aspects of "social" cell behavior, such as of adhesion-dependent growth, contact inhibition, cell polarity as well as as tissue and single cell geometry and mechanics. Clearly, cells are able to integrate these cues to attain their identity and positional information by impinging on YAP/TAZ through the Hippo pathway and cytoskeleton. The challenge is now discovering how all this is computed.

METHODS

Reagents, microfabrications and plasmids

Cell-permeable C3 transferase (Cytoskeleton Inc.) was used in serum-free conditions for MCF10A and hMSC, in complete medium for HMVEC. Y27632, Blebbistatin, Nocodazole were from Sigma. LatrunculinA was from SantaCruz. SwinholideA was from Merck. NSC23766 was from Tocris. Micropatterned glass slides were purchased from Cytoo SA; on every slide, square islands of different sizes were arrayed in quadrants, leaving 70mm of non-adhesive glass between each island; a control area evenly coated with fibronectin was also included to let cells attach without geometric constraints. Fibronectin-coated hydrogels were synthesized according to Tse et al., 2010. Micropost arrays were prepared according to du Roure et al., 2005; with microposts of 1mm in diameter and 3mm of center-to-center distance; elasticity of the micropillars was changed by modulating the amount of cross-linker (10% in the stiff micropillars, 5% in the elastic ones) and their length, as in Fu et al., 2010; in order to obtain nominal spring constants of >10,9 nN/mm for rigid micropillars, and 1,92 nN/mm for the elastic ones. HA-5SA-YAP1 was subcloned into pCSII-EF-MCS to produce lentiviral particles. 4SA-mTAZ cDNA was synthesized ad-hoc (GeneScript).

Cell lines, transfections and treatments

Mouse NmuMG cells were cultured in DMEM 10% FCS. Human MCF10A cells were cultured in DMEM/F12 with 5% HS freshly supplemented with Insulin, EGF,

Hydrocortisone and Cholera toxin. Human MDA-MB-231 were cultured in DMEM/F12 with 10% FBS. BM-derived hMSC and HMVEC-L were purchased from Lonza and cultured according to the manifacturer instructions. siRNA transfections were done with Lipofectamine RNAi-MAX (Invitrogen) in antibiotics-free medium according to manifacturer instructions.

Sequences of siRNAs are the following:

siRNA	SENSE STRAND SEQUENCE
YAP 1	GACAUCUUCUGGUCAGAGA dTdT
YAP 2	CUGGUCAGAGAUACUUCUU dTdT
TAZ 1	ACGUUGACUUAGGAACUUU dTdT
TAZ 2	AGGUACUUCCUCAAUCACA dTdT
LATS1 A	CACGGCAAGAUAGCAUGGA dTdT
LATS1 B	CAUACGAGUCAAUCAGUAA dTdT
LATS2 A	AAAGGCGUAUGGCGAGUAG dTdT
LATS2 B	GCCACGACUUAUUCUGGAA dTdT
Control	UUCUCCGAACGUGUCACGU dTdT

YAP/TAZ mix #1 is composed of oligos YAP1 and TAZ1; YAP/TAZ mix #2 is composed of oligos YAP2 and TAZ2; LATS1/2 mix A is composed of oligos LATS1A and LATS2A; LATS1/2 mix B is composed of oligos LATS1B and LATS2B.

DNA transfections were done with TransitLT1 (MirusBio). Lentiviral particles were prepared by transiently transfecting HEK293T cells with lentiviral vectors together with packaging vectors (pMD2-VSVG and psPAX2). Luciferase assays with the established YAP/TAZ-responsive reporter 4xGTIIC-lux (Mahoney et al., 2005) were as in Martello et al., 2010, and displayed as arbitrary units.

For hydrogels, 5,000-10,000 cells/cm^2 were seeded in drop; after attachment, the wells containing the hydrogels were filled with appropriate medium. hMSC and mammary cells were plated in growth medium and harvested for IF after 24hours; for luciferase and gene expression after 48 hours. For bone

differentiation assays, growth medium was changed with osteogenic differentiation medium 24 hours after seeding, and renewed every two days for a total of 8 days of differentiation. Bone differentiation was assayed by Alkaline Phosphatase staining (Sigma #85L2) and quantified with ImageJ software as follows: for each sample, at least five low magnification (20X) pictures were taken, and the alkaline phosphatase-positive area was determined with ImageJ as the number of blue pixels across the picture; this value was then normalized to the number of cells (Hoechst/nuclei) for each picture (Arbitrary Units). For adipogenic differentiation, growth medium was replaced with adipogenic induction medium 24 hours after seeding; cells were then subjected to cycles of 3 days of adipogenic induction and 1 day of adipogenic maintenance until harvesting at day 7 of differentiation. Adipogenic differentiation was assayed by Oil Red staining (Sigma) and quantified as the Oil Red-positive area normalized to the number of cells (Hoechst-positive nuclei) in a manner similar to that described for bone differentiation.

For micropatterns and micropost arrays, 40,000 HMVEC or hMSC cells were plated in 35mm dishes in growth medium. For immunofluorescence, cells were fixed 24 hours after plating. For HMVEC proliferation and apoptosis assays, cells were fixed 24 hours after plating (including 1hour incubation with BrdU in the case of proliferation assays) and processed according to TUNEL or BrdU detection kits (Promega DeadEnd and Roche Kit#1, respectively). The projected cell area of cells on fibronectin-coated glass slides and on microposts was determined with imageJ based on IF pictures of cells stained with anti-YAP/TAZ; the area of ECM contacted by cells was estimated by calculating that microposts (diameter 1mm) arrayed in

equilateral triangles (center-to-center 3mm) approximate 10% of the total surface covered by cells (projected cell area).

For drug treatments and IF, 10,000 cells/cm^2 were plated onto 8-well glass Lab-Tek chamberslides (Nunc) precoated for 1 hour at 37°C with 20mg/ml bovine Fibronectin (Sigma) in 1XPBS. Unless indicated otherwise, drug concentrations are indicated in the legend to Fig. 7A and 8A, and treatments lasted 4hours for IF, 6 hours for western blotting, and overnight for luciferase and gene expression assays. For serum stimulations, cells were incubated overnight without serum and then stimulated for 6 hours with 20% serum; for combined treatments, drugs were added together with 20% serum.

Antibodies, western blotting and immunofluorescence

Western blotting (WB) was carried out as in Dupont at al., 2009. Immunofluorescence (IF) was as in Morsut et al., 2010. Antibodies: anti-YAP/TAZ 1:200 for IF (sc101199 detecting both YAP and TAZ in WB), anti-phosphoS127-YAP (CST #4911), anti-LATS1 (CST #3477), anti-LATS2 (Abnova ab70565), anti-GAPDH (Millipore mAb374), anti-vinculin (VIN-11-5). Primary antibodies for IF were incubated overnight in PBS+0,1% Triton and 2% Goat Serum. Secondary antibodies were GAM Alexa488, GAM Alexa568 and GAR Alexa555 (Invitrogen). YOYO1, TOTO3 (Invitrogen) or Hoechst were used in combination with RNAse to counterstain nuclei. Alexa488-conjugated phalloidin (Invitrogen) was used 1:100 in 1% BSA to visualize F-actin microfilaments. Firm-setting anti-fade mounting medium was 10% Mowiol 4-88, 2,5% DABCO, 25% Glycerol, 0,1M Tris-HCl pH=8.5. Images were

acquired with a Leica SP2 confocal microscope equipped with a CCD camera. Cells seeded on microposts were observed in 1XPBS with a BioRad upright confocal microscope with water immersion long-range objectives. Pictures of cells seeded on small adhesive islands were rescaled to allow better appreciation of immunostainings. For quantifications of YAP/TAZ subcellular localizations, YAP/TAZ IF signal was scored as predominantly nuclear vs. evenly distributed/predominantly cytoplasmic in 150-200 cells for each experimental condition.

Real-time PCR

Cultures were harvested in Trizol (Invitrogen) for total RNA extraction, and contaminant DNA was removed by DNAseI treatment. cDNA synthesis was carried out with dT-primed MuMLV ReverseTrascriptase (Invitrogen). Real-time qPCR analyses were carried out on triplicate samplings of retrotranscribed cDNAs with RG3000 Corbett Research thermal cycler and analyzed with Rotor-Gene Analysis6.1 software. Expression levels are given relative to *GAPDH.* Sequences of primers are the following:

GENE	PRIMER NAME	PRIMER SEQUENCE
GAPDH	GAPDH F	CTCCTGCACCACCAACTGCT
	GAPDH R	GGGCCATCCACAGTCTTCTG
ANKRD1	ANKRD1 FOR	AGTAGAGGAACTGGTCACTGG
	ANKRD1 REV	TGGGCTAGAAGTGTCTTCAGAT
CTGF	CTGF F2	AGGAGTGGGTGTGTGACGA
	CTGF R2	CCAGGCAGTTGGCTCTAATC
LATS1	LATS1 L1	CTCTGCACTGGCTTCAGATG
	LATS1 R1	TCCGCTCTAATGGCTTCAGT
LATS2	LATS2 L1	ACATTCACTGGTGGGGACTC
	LATS2 R1	GTGGGAGTAGGTGCCAAAAA

Primers used for the molecular characterization of hMSC differentiation were as in Fu et al., 2010.

Biostatistical analysis

The statistical association between genes differentially expressed in mammary epithelial cells (MEC) cultivated on ECM of high/low stiffness (stiffness signature) and belonging to signal transduction pathways is assessed by an over-representation analysis approach using Fisher's exact test. Briefly, considering that there are S single-symbol-annotated genes on the stiffness signature, the over-representation of a pre-defined pathway signature is calculated as the hypergeometric probability of having α genes for a specific pathway in S, under the null hypothesis that they were picked out randomly from the N total genes of the microarray. Over-representation analysis has been conducted using one-sided Fisher's exact test (*phyper* function of R *stats* package; p-value<0.05) and considering 19621 single-symbol-annotated genes on the HG-U133 Plus2.0

microarray. P-values have been adjusted for False Discovery Rate (*p.adjust* function of R *stats* package; FDR<5%).

The stiffness signature has been derived from Supplementary Table 1 of Provenzano et al., 2009. The complete signature contains 1236 probe sets of the Affymetrix 430 2.0 mouse array accounting for 1015 single-symbol-annotated. MOE430 Plus2.0 probe Ids have been converted to the correspondent HG-U133 Plus2.0 probe sets using the NetAffx ortholog annotation file derived from the NCBI HomologoGene database (MOE430A Orthologs/Homologs Release 30, http://www.affymetrix.com/). This conversion table allows mapping orthologous probe sets (i.e. probe sets interrogating transcripts from orthologous genes) across two Affymetrix types of arrays. The 1236 mouse probe sets of the stiffness signature were converted into 1793 human probe sets corresponding to 807 single-symbol-annotated genes. Similarly, probe sets of all pathway signatures have been first converted into HG-U133 Plus2.0 probe sets, and then annotated as gene symbols using Bioconductor *hgu133plus2.db* package (release 2.3.5). Gene-sets of specific signaling pathways have been derived from: TGFba (Padua et al., 2008); TGFbb (Adorno et al., 2009); H-Ras and β-catenin (Bild et al., 2006); ERBB2 (Mackay et al., 2006); YAP (Zhao et al., 2008; Dong et al., 2007; Ota and Sasaki, 2008); YAP/TAZ (Zhang et al., 2009) ; WNT (DiMeo et al., 2009); Notch and NICD (Mazzone et al., 2010); MAL/SRFa (Descot et al., 2009); MAL/SRFb (Selvaraj and Prywes, 2004); NF-kB (Park et al., 2007). Genes of WNT and b-Catenin pathway lists were not represented in the stiffness signature.

The “YAP/TAZ signature” was published as supplemental table in Zhang et al., 2009. The second “YAP signature” of Figure 5A contains the genes commonly upregulated by YAP in human MCF10A cells, mouse NIH3T3 cells and mouse liver as obtain from the merging of data published in Zhao et al., 2008; Dong et al., 2007; Ota and Sasaki, 2008; Zhang et al., 2009).

REFERENCES

Adorno, M., Cordenonsi, M., Montagner, M., Dupont, S., Wong, C., Hann, B., Solari, A., Bobisse, S., Rondina, M.B., Guzzardo, V., Parenti, A. R., Rosato, A., Bicciato, S., Balmain, A. and Piccolo S. (2009) A Mutant-p53/Smad complex opposes p63 to empower TGFbeta-induced metastasis. *Cell* **137**, 87-98.

Arnadottir, J. and Chalfie, M. (2010) Eukaryotic mechanosensitive channels. *Annu Rev Biophys* **39**, 111-137.

Badouel, C. and McNeill, H. (2011) SnapShot: The hippo signaling pathway. *Cell* **145**, 484-484.

Basu, S., Totty, N. F., Irwin, M. S., Sudol M. and Downward J. (2003) Akt phosphorylates the Yes-associated protein, YAP, to induce interaction with 14-3-3 and attenuation of p73-mediated apoptosis. *Mol Cell* **11**, 11-23.

Bild, A. H., Yao, G., Cheng, J. T., Wang, Q., Potti, A., Chasse, D., Joshi, M. B., Harpole, D., Lancaster, J. M., Berchuck, A., Olson, J. A., Marks, J. R., Dressman, H. K., West, M. and Nevins, J. R. (2006) Oncogenic pathway signatures in human cancers as a guide to targeted therapies. *Nature* **439**, 353-357.

Butcher, D., T., Allison, T. and Weaver, V. M. (2009) A tense situation: forcing tumor progression. *Nat Rev Cancer* **9**, 108-122.

Callus, B. A., Verhagen, A. M. and Vaux, D.L. (2006) Association of mammalian sterile twenty kinases, Mst1 and Mst2, with hSalvador via C-terminal coiled-coil domains, leads to its stabilization and phosphorylation. *FEBS J* **273**, 4262-4276.

Camargo, F. D., Gokhale, S., Johnnidis, J. B., Fu, D., Bell., G. W., Jaenisch, R. and Brummelkamp, T. R. (2007) YAP1 increases organ size and expands undifferenziated progenitor cells. *Curr Biol* **17**, 2054-2060.

Chan, E. H., Nousianen, M., Chalamalasetty, R. B., Schafer, A., Nigg, E. A. and Silljè, H. H. (2005) The Ste20-like kinase Mst2 activates the human large tumor suppressor kinase Lats1. *Oncogene* **24**, 2076-2086.

Chen, C. S., Mrksich, M., Huang, S., Whitesides, G. M. and Ingber, D. E. (1997) Geometric control of cell life and death. *Science* **276**, 1425-1428.

Chen, Z., Friedrich, G. A. and Soriano, P. (1994) Transcriptional enhancer factor 1 distruption by retroviral gene trap leads to heart efects and embryonic lethality in mice. *Genes Dev* **8**, 2293-2301.

Choi, C. K., Breckendridge, M. T. and Chen, C. S. (2010) Engineered materials and the cellular microenvironment: a strengthening interface between cell biology and bioengineering. *Trends Cell Biol* **20**, 705-714.

Chowdhury, F., Na, S., Li, D., Poh, Y. C., Tanaka, T. S., Wang, F. and Wang, N. (2010) Material properties of the cell dictate stress-induced spreading and differentiation in embryonic stem cell. *Nat Mater* **9**, 82-88.

Cordenonsi, M., Zanconato, F., Azzolin, L., Forcato, M., Rosato, A., Frasson, C., Inui, M., Montagner, M., Parenti, A. R., Poletti, A., Daidone, M. G., Dupont, S., Basso, G., Bicciato, S. and Piccolo, S. (2011) The Hippo transducer TAZ confers cancer stem cell-related traits on breast cancer cells. *Cell* **147**, 759-772.

Cowel, C. F., Yan, I.K., Eiseler, T., Leightner, A.C., Doppler, H. and Storz, P. (2009) Loss of cell-cell contacts induces NF-kB via RhoA-mediated activation of protein kinase D1. *J Cell Biochem* **106**, 714-728.

Delmas, P. (2004) Polycistins: from mechanosensation to gene regulation. *Cell* **118**, 145-148.

Densham, R. M., O'Neill, E., Munro, J., Konig, I., Anderson, K., Kolch, W. and Olson, M. F. (2009) MST kinases monitor actin cytoskeletal integrity and signal via c-Jun N-terminal kinase stress-activated kinase to regulate p21Waf1/Cip1 stability. *Moll Cell Biol* **29**, 6380-6390.

Descot, A., Hoffmann, R., Shaposhnikov, D., Reschke, M., Ullrich, A. and Posern, G. (2009) Negative regulation of the EGFR-MAPK cascade by actin-MAL-mediated Mig6/Errfi-1 induction. *Mol Cell* **35**, 291-304.

DiMeo, T. A., Anderson, K., Phadke, P., Fan, C., Perou, C. M., Naber, S. and Kuperwasser, C. (2009) A novel lung metastasis signature links Wnt signaling with cancer cell self-renewal and epithelial-mesenchymal transition in basal-like breast cancer. *Cancer Res* **69**, 5364-5373.

Dong, J., feldmann, G., Huang, J., Wu, S., Zhang, N., Comerford, S. A., Gayyed, M. F., Anders, R. A., Maitra, A. and Pan, D. (2007) Elucidation of a universal size-control mechanism in Drosophila and mammals. *Cell* **130**, 1120-1133.

Dupont, S., Mamidi, A., Cordenonsi, M., Montagner, M., Zacchigna, L., Adorno, M., Martello, G., Stinchfield, M.J., Soligo, S., Morsut, L., Inui M., Moro, S., Modena, N., Argenton, F., Newfeld, S.J. and Piccolo, S. (2009) FAM/USP9x, a deubiquitinating enzyme essential for TGFbeta signaling, controls Smad4 monoubiquitination. *Cell* **136**, 123-135.

Du Roure, O. *et al.* (2005) Force mapping in epithelial cell migration. *Proc Natl Acad Sci U S A* **102**, 2390-2395.

Eyckmans, J., Boudou, T., Yu, X. and Chen, C. S. (2011) A Hitchhiker's Guide to Mechanobiology. *Dev Cell* **21**, 35-47.

Engler, A. J., Sen, S., Sweeney, H. L. and Disher D. E. (2006) Matrix elasticity directs stem cell lineage specification. *Cell* **126**, 677-689.

Folkman, J. and Moscona, A. (1978) Role of cell shape in growth control. *Nature* **273**, 345-349.

Friedland, J. C., Lee, M. H. and Boettiger, D. (2009) Mechanically activated integrin switch control alpha5beta1 function. *Science* **323**, 642-644.

Fu, J., Wang, Y. K., Yang, M. T., Desai, R. A., Yu, X., Liu, Z., and Chen, C. S. (2010) Mechsnical regulation of cell function with geometrically modulated elastomeric substrates. *Nat Methods* **7**, 733-736.

Gao, L., McBeath, R., and Chen, C. S. (2010) Stem cell shape regulates a chondrogenic versus myogenic fate through Rac1 and N-cadherin. *Stem Cells* **28**, 564-572.

Garcia-Fernandez, B., Gaspar, P., Bras-Pereira, C., Jezowska, B., Raquel-Rebelo, S and Janody, F. (2011) Actin-capping protein and the Hippo pathway regulate F-actin and tissue growth in Drosophila. *Development* **138**, 2337-2346.

Gilbert, P. M., Havenstrite, K. L., Magnusson, K. E., Sacco, A., Leonardi, N. A., Kraft, P., Nguyen, N. K., Thrun, S., Lutolf, M. P. and Blau, H. M. (2010) Substrate elasticity regulates skeletal muscle stem cell self-renewal in culture. *Science* **329**, 1078-1081.

Hahn, C. and Schwartz, M. A. (2009) Mechanotransduction in vascular physiology and atherogenesis. *Nat Rev Mol Cell Biol* **10**, 53-62.

Halder, G. and Johnson, R. L. (2011) Hippo signaling: growth control and byond. *Development* **138**, 9-22.

Harvey, K. F., Pfleger, C. M. and Hariharan, I. K. (2003) The Drosophila Mst ortholog, hippo, restricts growth and cell proliferation and promotes apoptosis. *Cell* **114**, 457-467.

Hoffman, B. D., Grashoff, C. and Schwartz, M. A. (2011) Dynamic moleclular processes mediate cellular mechanotransduction. Nature **475**, 316-323.

Holst, J., Watson, S., Lord, M. S., Eamegdool, S. S., Bax, D. V., Nivison-Smith, L. B., Kondyurin, A., Ma, L., Oberhauser, A. F., Weiss, A. S. and Rasko, J. E. (2010) Substrate elasticity provides mechanical signals for the expansion of hematopoietic stem and progenitor cells. *Nat Biotechnol* **28**, 1123-1128.

Hossain, Z., Ali, S. M., Ko, H. L., Xu, J., Ng, C. P., Guo, K., Ponniah, S., Hong, W. and Hunziker, W. (2007) Glomerulocystic kidney disease in mice with a targeted inactivation of Wwtr1. *Proc Natl Acad Sci USA* **104**, 1631-1636.

Huang, J., Wu, S., Barrera, J., Matthews, K., and Pan, D. (2005) The Hippo signaling pathway coordinately regulates cell proliferation and apoptosis by inactivating Yorkie, the Drosophila Homolog of YAP. *Cell* **122**, 421-434.

Jaalouk, D. E. and Lammerding, J. (2009) Mechanotransducion gone awry. *Nature Rev Mol Cell Biol* **10**, 63-73.

Jia, J., Zhang, W., Wang, B., Trinko, R. and Jiang, J. (2003) The Drosophila Ste20 family kinase dMST functions as a tumor suppressor by restricting cell proliferation and promoting apoptosis. *Genes Dev* **17**, 2514-2519.

Justice, R. W., Zlian, O., Woods, D. F., Noll, M., and Bryant, P. J. (1995) The Drosophila tumor suppressor gene warts encodes a homolog of human myotonic dystrophy kinase and is required for the control of cell shape and proliferation. *Genes Dev* **9**, 534-546.

Kanai, F., Marignani, P. A., Sarbassova, D., Yagi, R., Hall , R. A., Donowitz, M., Hisaminato, A., Fujiwara, T., Ito, Y., Cantley, L. C. and Yaffe, M. B. (2000) TAZ: a novel transcriptional co-activators regulated by interaction with 14-3-3 and PDZ domains protein. *Embo J* **19**, 6778-6791.

Kanchanawong, P., Shtengel, G., Pasapera, A. M., Ramko, E. B., Davidson, M. W., Hess, H. F. and Waterman, C. M. (2010) Nanoscale architecture of integrin-based cell adhesions. *Nature* **468**, 580-584.

Kumar, A., Khandelwal, N., Malya, R., Reid, m. B. and Boriek, A. M. (2004) Loss of dystrophin causes aberrant mechanotransduction in skeletal muscle fibers. *FASEB J* **18**, 102-113.

Lai, Z. C., Wei, X., Shimiuz, T., Ramos, E., Rohrbaugh, M., Nikolaidis, N., Ho, L. L. and Li, Y. (2005) Control of cell proliferation and apoptosis by mob as tumor suppressor, mats. *Cell* **120**, 675-685.

Lansman, J. B., Hallam, T. J. and Rink, T. J. (1987) Single stretch-activated ion channels in vascular endothelial cells as mechanotransducers? *Nature* **325**, 811-813.

Lee, K. P., Lee, J. H., Kim, T. S., Kim, T. H., Park, H. D., Byun, J. S., Kim, M. C., Jeong, W. I., Calvisi, D. F., Kim, J. M. and Lim, D. S. (2010) The Hippo-Salvador pathway restrains hepatic oval cell proliferation, liver size, and liver tumorigenesis. *Proc Natl Acad Sci USA* **107**, 8248-8253.

Lei, Q. Y., Zhang, H., Zhao, B., Zha, Z. Y., Bai, F., Pei, X. H., Zhao, S., Xiong, Y. and Guan, K. L. (2008) TAZ promotes cell proliferation and epithelial-mesenchymal transition and is inhibited by the hippo pathway. *Mol Cell Biol* **28**, 2426-2436.

Levental, K. R., Yu, H., Kass, L., Lakins, J. N., Egeblad, M., Erler, J. T., Fong, S. F., Csiszar, K., Giaccia, A., Weninger, W., Yamauchi, M., Gasser, D. L. and Weaver V. M. (2009) Matrix crosslinking forces tumor progression by enhacing integrin signaling. *Cell* **139**, 891-906.

Liu, F., Mih, J. D., Shea, B. S., Kho, A. T., Sharif, A. S., Tager, A. M. and Tschumperlin, D. J. (2010) Feedback amplification of fibrosis through matrix stiffening and COX-2 suppression. *J Cell Biol* **190**: 693-706.

Liu, C. Y., Zha, Z. Y., Zhou, X., Zhang, H., Huang, W., Zhao, D., Li, T., Chan, S.W., Lim, C. J., Hong, W., Zhao, S., Xiong, Y., Lei, Q. Y. and Guan, K. L. (2010) The Hippo tumor pathway promotes TAZ degradation by phosphorylating a phosphodegron and recruiting the SCF{beta}-TrCP E3 ligase. *J Biol Chem* **285**, 37159-37169.

Mackay, A., Jones, C., Dexter, T., Silva, R. L., Bulmer, K., Jones, A., Simpson, P., Harris, R. A., Jat, P. S., Neville, A. M., Reis, L. F., Lakhani, S. R. and O'Hare, M. J. (2003) cDNA microarray analysis of genes associated with ERBB2 (HER2/neu) overexpression in human mammary luminal epithelial cells. *Oncogene* **22**, 2680-2688.

Mahoney, W. M., Jr., Hong, J. H., Yaffe, M. B. & Farrance, I. K. (2005) The transcriptional co-activator TAZ interacts differentially with transcriptional enhancer factor-1 (TEF-1) family members. *Biochem J* **388**, 217-225.

Makita, R., Uchijima, Y., Nishiyama, K., Amano, T., Chen, Q., Takeuchi, T., Mitani, A., Nagae, T., Yatomi, Y., Aburatani, H., Nakagawa, O., Small, E. V., Cobo-Stark, P., Igarashi, P., Murakami, M., Tominaga, J., Sato, T., Asano, T., Kurihara, Y. and Kurihara, H. (2008) Multiple renal cysts, urinary concentration defects, and pulmonary emphysematous changes in mice lacking TAZ. *Am J physiol Renal Physiol* **294**, F542-F553.

Marinissen, M.J, Chiariello, M., Tanos, T., Bernard, O., Narumiya, S. and Gutkind, J.S. (2004) The small GTP-binding protein RhoA regulates c-Jun by ROCK-JNK signaling axis. *Mol Cell* **14**, 29-41.

Martello, G., Rosato, A., Ferrari, F., Manfrin, A., Cordenonsi, M., Dupont, S., Enzo, E., Guzzardo, V., Rondina, M., Spruce, T., Parenti, A. R., Daidone, M. G., Bicciato, S. and Piccolo, S. (2010) A MicroRNA targeting dicer for metastasis control. *Cell* **141**, 1195-1207.

Mauviel, A., Nallet-Staub, F. and Varelas X. (2011) Integrating developmental signals: a hippo in the (path)way. *Oncogene* doi:10.1038/onc.2011.363.

Mammoto, A. and Ingberg, D. E.(2009) Cytoskeletal control of growth and cell fate switching. *Curr Opin Cell Biol* **21**, 864-870.

Mammoto, A. and Ingberg, D. E. (2010) Mechanical control of tissue and organ development. *Development* **137**, 1407-1420.

Mazzone, M., Selfors, L. M., Albeck, J., Overholtzer, M., Sale, S., Carroll, D. L., Pandya, D., Lu, Y., Mills, G. B., Aster, J. C., Artavanis-Tsakonas, S. and Brugge, J. S. (2010) Dose-dependent induction of distinct phenotypic responses to Notch pathway activation in mammary epithelial cells. *Proc Natl Acad Sci U S A* **107**, 5012-5017.

McBeath, R., Pirone, D. M., Nelson, C. M., Bhadriraju, K. and Chen, C. S. (2004) Cell shape, cytoskeletal tension, and RhoA regulate stem cell lineage commitment. *Dev Cell* **6**, 483-495.

McCartney, B. M., Kulikauskas, R. M., LaJeunesse, D. R. and Fehon, R. G. (2000) The neurofibromatosis-2 homologue, Merlin, and the tumor suppressor expanded function together in drosophila to regulate cell proliferation and differentiation. *Development* **127**, 1315-1324.

Miralles, F., Posern, G., Zaromytidiu, A. I. and Treisman, R. (2003) Actin dinamic control SRF activity by regulation of its cofactor MAL. *Cell* **113**, 329-342.

Morin-Kensicki, E. M., Boone, B. N., Howell, M., Stonebraker, J. R., Teed, J., Alb, J. G., Magnuson, T. R., O'Neal, W. and Milgram, S. L. (2006)Defects in yolk salc vasculogenesis, chorioallantoic fusion, and embryonic axis elongation in mice with targeted disruption of Yap65. *Mol Cell Biol* **26**, 77-87.

Morsut, L., Yan, K. P., Enzo, E., Aragona, M., Soligo, S. M., Wendling, O., Mark, M., Khetchoumian, K., Bressan, G., Chambon, P., Dupont, S., Losson, R. and Piccolo, S. (2010) Negative control of Smad activity by ectodermin/Tif1gamma patterns the mammalian embryo. *Development* **137**, 2571-2578.

Moustakas, A. and Heldin, C. H. (2008) Dynamic control of TGF-b signaling and its links to the cytoskeleton. *FEBS Lett* **582**, 2051-2065.

Nienhaus, U., Aegerter-Wilmsen, T. and Aegerter, C. M. (2009) Determination of mechanical stress distribution in Drosophila wing discs using photoelasticity. *Mech Dev* **126**, 942-949.

Oka, T., Mazack, V. and Sudol, M. (2008) Mst2 and Lats kinases regulate apoptotic function of Yes kinase-associated protein (YAP). *J Biol Chem* **283**, 27534-27546.

Oka, T., Remue, E., Meerschaert, K., Vanloo, B., Boucherie, C., Gfeller, D., Bader, G. D., Sidhu, S. S., Vandekerchove, J., Gettemans, J. and Sudol, M. (2010) functional complexes between YAP2 and ZO-2 are PDZ domain-dependent, and regulate YAP2 nuclear localization and signalling. *Biochem J* **432**, 461-472.

Olson, E. N. and Nordheim, A. (2010) Linking actin dynamics and gene transcription to drive cellular motile functions. *Nature Rev Mol Cell Biol* **11**, 353-365.

Ota, M. and Sasaki, H. (2008) Mammalian Tead proteins regulate cell proliferation and contact inhibition as transcriptional mediators of hippo signaling. *Development* **135**, 4059-4069.

Padua, D., Zhang, X. H., Wang, Q., Nadal, C., Gerals, W. L., Gomis, R. R. and Massaguè, J. (2008) TGFbeta primes breast tumors for lung metastasis seeding through angiopoietin-like 4. *Cell* **133**, 66-77.

Pan, D. (2010) The Hippo Signaling Pathway in Development and Cancer. *Dev Cell* **19**, 491-505.

Park, B. K., Zhang, H., Zeng, Q., Dai, J., Keller, E. T., Giordano, T., Gu, K., Shah, V., Pei, L., Zarbo, R. J., McCauley, L., Shi, S., chen, S. and Wang, C. Y. (2007) NF-kappaB in breast cancer cells promotes osteolytic bone metastasis by inducing osteoclastogenesis via GM-CSF. *Nat Med* **13**, 62-69.

Pece, S., Tosoni, D., Confalonieri, S., Mazzarol, G., Vecchi, M., Ronzoni, S., Bernard, L., Viale, G., Pelicci, P. G. and Di Fiore, P. P. (2010) Biological and molecular heterogeneity of breast cancers correlates with their cancer stem cell content. *Cell* **140**, 62-73.

Provenzano, P. P., Inman, D. R., Eliceiri, K. W. and Keely, P. J. (2009) Matrix density-induced mechanoregulation of breast cell phenotype, signaling and gene expression through a FAK-ERK linkage. *Oncogene* **28**, 4326-4343.

Provenzano, P. P. and Keely P. J. (2011) Mechanical signaling through the cytoskeleton regulates cell proliferation by coordinated focal adhesion and Rho GTPase signaling. *J Cell Sci* **124**, 1195-1205.

Remue, E., Meerschaert, K., Oka., T., Boucherie, C., Vandekerckhove, J., Sudol, M., and Gettemans, J. (2010) TAZ interacts with zona occludens-1 and -2 proteins in a PDZ-1 dependent manner. *FEBS Lett* **584**, 4175-4180.

Ren, F., Zhang, L. and Jiang, J (2010). Hippo signaling regulates Yorkie nuclear localization and activity through 14-3-3 dependent and independent mechanisms. *Dev Biol* **337**, 303-312.

Sansores-Garcia, L., Bossuyt, W., Wada, K. I., Yonemura, S., Tao, C., Sasaki, H. and Halder, G. (2011) Modulating F-actin organization induces organ growth by affecting the Hippo pathway. *EMBO J* **30**, 2325-2335.

Sawada, Y., Tamada, M., Dubin-Thaler, B. J., Cherniavskaya, O., Sakai, R., Tanaka, S., Sheetz, M. P. (2006) Force sensing by mechanical extension of the Src family kinase substrate p130Cas. *Cell* **127**, 1015-1026.

Schlegelmilch, K., Mohseni, M., Kirak, O., Pruszak, J., Rodriguez, J.R., Zhou D., Kreger, B. T., Vasioukhin, V., Avruch, J., Brummelkamp, T. R. and Camargo, F. D. (2011) Yap1 acts downstream of alfa-catenin to control epidermal proliferation. *Cell* **144**, 782-795.

Schwank. G. and Basler, K. (2010) Regulation of organ growth by morphogen gradients. *Cold Spring Harb Perspect Biol* **2**, a001669.

Schwartz, M. A. (2010) Integrins and extracellular matrix in mechanotransduction. *Cold Spring Harb Perspect Biol* **2**, a005066.

Selvaraj, A. and Prywes, R. (2004). Expression profiling of serum inducible genes identifies a subset of SRF target genes that are MKL dependent. *BMC Mol Biol* **5**, 13.

Silvis, M. R., Kreger, B. T., Lien, W. H., Klezovitch, O., Rudakova, G. m. and camargo, F. D. (2011) Alfa-catenin is a tumor suppressor that control cell accumulation by regulating the localization and activity of the transcriptional coactivator Yap1. *Sci Signal* **4**, ra33.

Skouloudaki, K., Puetz, M., Simons, M., Courbard, J. R., Boehlke, C., Hartleben, B., Engel, C., Moeller, M. J., Englert, C., Bollig, F., Schafer, T., Ramachandran, H., Mlodzik, M., Huber, T. B., Kuehn, E. W., Kim, E., Kramer-Zucker, A. and Walz, G. (2009) Scribble participates in Hippo signaling and is required for normal zebrafish pronephoros development. *Proc Natl Acad Sci USA* **106**, 8579-8584.

Sordella, R., Jiang, W., Chen, G. C., Curto, M. and Settleman, J. (2003) Modulation of Rho GTPase signaling regulates a switch between adipogenesis and myogenesis. *Cell* **113**, 147-158.

Tarbell, J.M. and Ebong, E. E. (2008) The endothelial glycocalix: a mechano-sensor and –transducer. *Sci Signal* **1**, Issue 40 pt8.

Thiery, J. P., Acloque, H., Huang, R. Y. and Nieto, M. A. (2009) Epithelial-mesenchymal transition in development and disease. *Cell* **139**, 871-890.

Tse, J. R. and Engler, A. J. (2010) Preparation of hydrogel substrates with tunable mechanical properties. *Curr Protoc Cell Biol* Chapter **10**, Unit 10 16.

Tzima, E., Irani-Tehrani, M., Kiosses, W. B., Dejana, E., Schultz, D. A., Engelhardt, B., Cao, G., DeLisser, H. and Schwartz, M. A. (2005) A mechanosensory complex that mediates the endothelial cell response to fluid shear stress. *Nature* **437**, 426-431.

Udan, R. S., Kango-Singh, M., Nolo, R., Tao, C. and Halder, G. (2003) Hippo promotes prolifertion arrest and apoptosis in the Salvador/Warts pathway. *Nat Cell Biol* **5**, 914-920.

Vartiainen, M. K., Guettler, S., Larijani, B. and Treisman, R. (2007) Nuclear actin regulates dynamic subcellular localization and activity of the SRF cofactor MAL. *Science* **316**, 1749-1752.

Vogel, V. and Sheetz, M. (2006) Local force and geometry sensing regulate cell functions. *Nature Rev Mol Cell Biol* **7**, 265-275.

Winter, C. G., Wang, B., Ballew, A., Royou, A., Karess, R., Axelrod, J. D. and Luo, L. (2001) Drosophila Rho-associated kinase (Drok) links Frizzled-mediated planar cell polarity signaling to the actin cytoskeleton. *Cell* **105**, 81-91.

Wozniak, M. A. and Chen C. S. (2009) Mechanotransduction in development: a growing role for contractility. *Nature Rev Mol Cell Biol* **10**, 34-43.

Wu, S., Huang, J., Dong, J. and Pan, D. (2003) hippo encodes a Ste-20 family protein kinase that restricts cell proliferation and promotes apoptosis in conjuction with salvador and warts. *Cell* **114**, 445-456

Xu, T., Wang, W., Zhang, S., Stewart, R. A. and Yu, W. (1995) Identifying tumor suppressor in genetic mosaics: the Drosophila lats gene encodes a putative protein kinase. *Development* **121**, 1053-1063.

Zhang, H., Liu, C. Y., Zha, Z. Y., Zhao, B., Yao, J., Zhao, S., Xiong, Y., Lei, Q. Y. and Guan, K. L. (2009) TEAD transcription factors mediate the function of TAZ in cell growth and epithelial-mesenchymal transition. *J Biol Chem* **284**, 13355-13362.

Zhang, H., Pasolli, H. A. and Fuchs, E. (2011) Yes-associated protein (YAP) transcriptional coactivator functions in balancing growth and differentiation in skin. *Proc Natl Acad Sci USA* **108**, 2270-2275.

Zhao, B., Li, L., Lu, Q., Wang, L. H., Liu, C. Y., Lei, Q, and Guan, K. L.(2011b) Angiomotin is a novel Hippo pathway component that inhibits YAP oncoprotein. *Genes Dev* **25**, 51-63.

Zhao, B., Li, L., Tumaneg, K., Wang, C. Y. and Guan, K. L. (2010) A coordinated phosphorilation by Lats and CK1 regulates YAP stability through SCF(beta-TRCP). *Genes Dev* **25**, 51-63.

Zhao, B., Tumaneng, K. and Guan, K. L. (2011a) The Hippo pathway in organ size control, tissue regeneration and stem cell self-renewal. *Nat Cell Biol* **13**, 877-883.

Zhao, B., Ye, X., Yu, J., Li, L., Li, W., Li, S., Yu, J., Lin, J. D., Wang, C. Y., Chinnaiyan, A. M., Lai, Z. C. and Guan, K. L. (2008) TEAD mediates YAP-dependent gene induction and growth control. *Genes Dev* **22**, 1962-1971.

Zhao, B., Wei, X., Li, W., Udan, R. S., Yang, Q., Kim, J., Ikenoue, T., Yu, J., Li, L., Zheng, P., Ye, K., Chinnaiyan, A., Halder, G., Lai, Z. C. and Guan, K. L.(2007) Inactivation of YAP oncoprotein by the Hippo pathway is involved in cell contact inhibition and tissue growth control. *Genes Dev* **21**, 2747-2761.

Zhou, D., Conrad, C., Xia, F., Park, J. S., Payer, B., Yin, Y., Lauwers, G. Y., Thasier, W., Lee, J. T., Avruch, J. and Bardeesy, N. (2009) Mst1 and Mst2 maintain hepatocyte quiescence and suppress hepatocellular carcinoma development through inactivation of the Yap1 oncogene. *Cancer Cell* **16**, 425-438.

Ziegler, W. H., Gingras, A. R., Critchley, D. R. and Emsley, J. (2008) Integrin connections to the cytoskeleton through talin and vinculin. *Biochem Soc Trans* **36**, 235-239.

Varelas, X., Samavarchi-Tehrani, P., Narimatsu, M., Weiss, A., Cockburn, K., Larsen B. G., Rossant, J. and Wrana, J. L. (2010) The Crumbs complex couples cell density sensing to Hippo-dependent control of the TGF-beta-SMAD pathway. *Dev Cell* **19**, 831-844.

Wada, K.I., Itoga, K., Okano, T., Yonemura, S. and Sasaki H. (2011) Hippo pathway regulation by cell morphology and stress fibers. *Development* **138**, 3907-3914.

Watt, F.M. (1998) Epidermal stem cells: markers, patterning and the control of stem cell fate. *Philos Trans R Soc Lond B Biol Sci* 353, 831-837.

FIGURE

Figure 1. Cellular mechanosensing and mechanoresponse

A) Biological components acting as cellular mechanosensors, schematically depicted in a representative cell. **A |** Stretc-activated ion channels in the plasma membrane open in response to membrane strain and allow the influx of calcium and other ions. **B |** In endothelial cells, the glycocalix, a layer of carbohydrate rich proteins on the cell surface, can mediate mechanostransduction signalling in response to fluid shear stress. **C, D |** Cell-cell junctional receptors or ECM-cell focal adhesion allow cells to probe their environments. **E |** Force-induced unfolding of ECM proteins, such as fibronectin, can initiate mechanotransduction signalling outside the cell. **F |** Intracellular strain can induce conformational changes in cytoskeletal elements such as filaments, crosslinkers or motor proteins, thereby changing binding affinities to specific molecules and activating signalling pathways. **G |** The nucelus itself has been proposed to act as mechanosensor. Intracellular deformation can alter chromatin conformation and modulate access to transcription factors or transcriptional machinery. **H |** Compression of the intercellular space can alter the effective concentration of autocrine and paracrine signaling molecules (from Jaalouk and Lammerding 2009).

B) Global regulation of cell function. This diagram shows the steps in mechanosensing over time involve periodic testing of the substrate, substrate modification and changes in cellular protein content. Initially, cells will sense the mechanical features of their environment, which will cause rapid motility and signalling responses. As the cell pulls on the environment, it will modify the ECM and will create new signals, such as those originating from fibronectin unfolding. Intracellular signals will alter the expression pattern of the cell and, over time, the cellular forces and cellulary generated matrices will change the cell shape. At any stage, extracellular signals, such as hormones or external mechanical stimuli, can cause acute changes that will set off a further round of cell and matrix modifications (from Vogel and Sheetz, 2006).

FIGURE 1

A

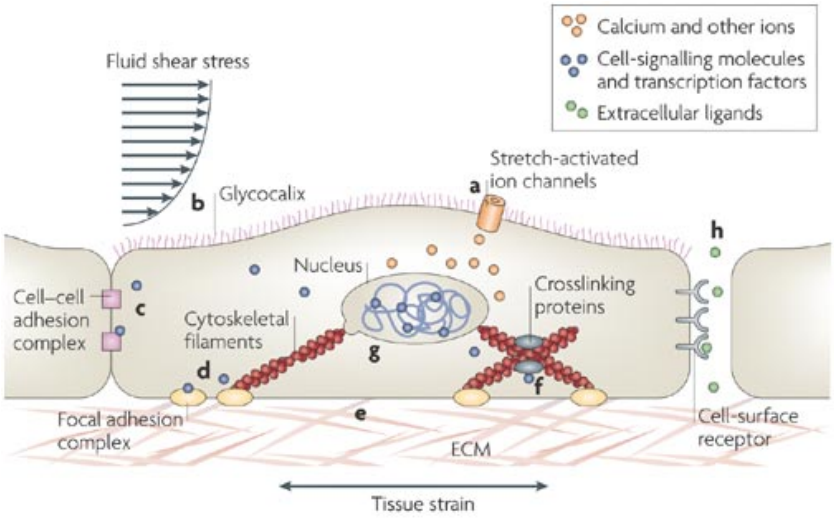
Calcium and other ions
Cell-signalling molecules and transcription factors
Extracellular ligands
Fluid shear stress
b
Glycocalix
a
Stretch-activated ion channels
h
Nucleus
Cell–cell adhesion complex
c
Cytoskeletal filaments
Crosslinking proteins
g
d
f
e
Focal adhesion complex
ECM
Cell-surface receptor
Tissue strain

B

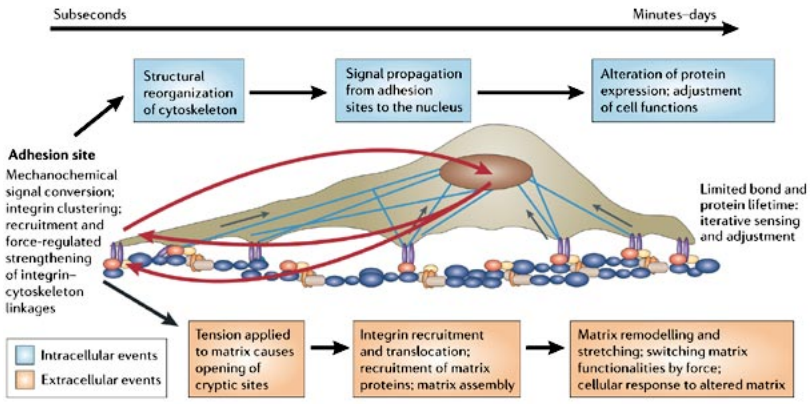
Subseconds
Minutes–days
Structural reorganization of cytoskeleton
Signal propagation from adhesion sites to the nucleus
Alteration of protein expression; adjustment of cell functions
Adhesion site
Mechanochemical signal conversion; integrin clustering; recruitment and force-regulated strengthening of integrin–cytoskeleton linkages
Limited bond and protein lifetime: iterative sensing and adjustment
Intracellular events
Extracellular events
Tension applied to matrix causes opening of cryptic sites
Integrin recruitment and translocation; recruitment of matrix proteins; matrix assembly
Matrix remodelling and stretching; switching matrix functionalities by force; cellular response to altered matrix

Figure 2. Cells are tuned to the materials properties of their matrix

A) All cells, are exposed to forces and tension that is genereted locally by cell-cell or cell-ECM interactions and that influences cell function through actomyosin contratility and actin dynamics. Moreover, each cell type is specifically tuned to the specific tissue in which it resides. The brain, for instance, is infinitely softer than bone tissue. Consequently, neural cell growth, survival, differentiation and morphogenesis are optimally supported by interaction with a soft matrix. Following transformation, breast tissue becomes progressively stiffer and tumor cells become significantly more contractile and hyper-responsive to matrix compliance cues (from Butcher et al., 2009). Solid tissue exhibit a range of stiffness, as measured by the elastic modulus.

B) The in vitro gel system allow for control of the elasticity of microenvironment *(E)* through crosslinking, control of cell adhesion by covalent attachment of collagen-I, and control of thickness, *h*. Naive MSCs are initially small and round but develop increasingly branched, spindle, or polygonal shapes when grown on matrices respectively in the range typical of ~E-brain (0.1-1 kPa), ~E-muscle (8-17 kPa), or stiff crosslinked-collagen matrices (25-40 kPa). Scale bar is 20 μm (from Engler et al., 2006).

FIGURE 2

A

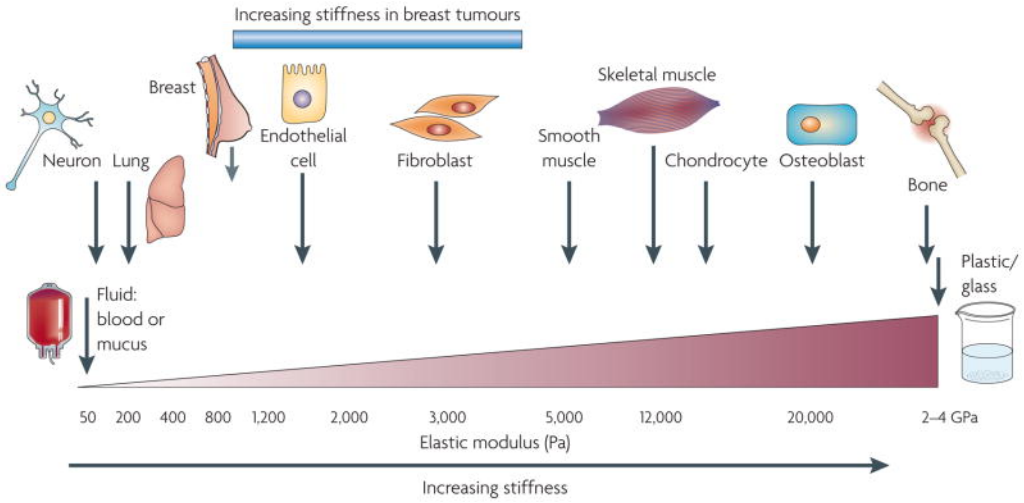
Increasing stiffness in breast tumours
Breast
Endothelial cell
Skeletal muscle
Smooth muscle
Chondrocyte
Osteoblast
Bone
Neuron
Lung
Fibroblast
Plastic/ glass
Fluid: blood or mucus
50
200
400
800
1,200
2,000
3,000
5,000
12,000
20,000
2–4 GPa
Elastic modulus (Pa)
Increasing stiffness

B

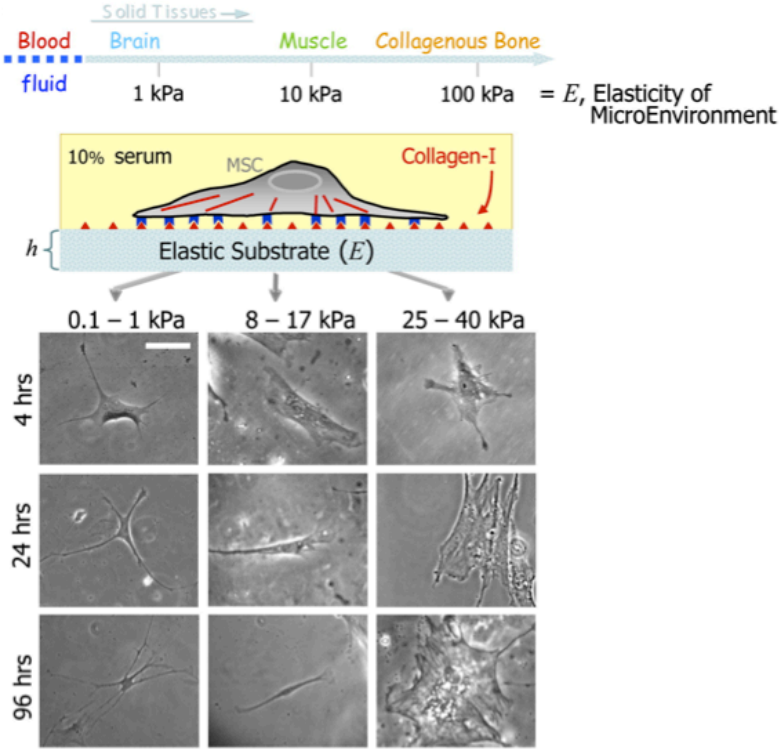
Solid Tissues
Blood
fluid
Brain
Muscle
Collagenous Bone
1 kPa
10 kPa
100 kPa
= E, Elasticity of MicroEnvironment
10% serum
MSC
Collagen-I
h
Elastic Substrate (E)
0.1 – 1 kPa
8 – 17 kPa
25 – 40 kPa
4 hrs
24 hrs
96 hrs

Figure 3. The Hippo signaling pathway in *Drosophila*

A) Schematics of the Hippo pathway in *Drosophila*. Pointed and blunt arrowheads indicate activating or inhibitory interactions, respectively. Direct biochemical interactions are indicated by solid lines or drawn as proteins in direct contact with each other, whereas dashed lines indicate unknown mechanisms. The core of the Hippo pathway is comprised of a series of phosphorylation events that lead to the inhibition of the transcriptional coactivator Yorkie (Yki). Initially, Hippo (Hpo) forms a complex with Salvador (Sav) to phosphorylate and activate Warts (Wts) that, in association with Mats, phosphorylate and inhibit Yki which is bind to 14-3-3 proteins that restricting Yki to the cytoplasm. Without inhibition from the Hippo pathway, Yki translocates into the nucleus, where it associates with the transcription factor Scalloped (Sd) to induce the expression of genes promoting proliferation. The atypical cadherins, Fat and Dachsous (Ds), are thought to act as receptor and ligand. Fat inhibits the atypical myosin Dachs, which binds Wts to induce its degradation. Dachs localization and activity are regulated by the Approximated (App). Fat also recruits Expanded (Ex) to the apical surface. Ex, with Merlin (Mer) and Kibra, promotes Hippo and Wts activation. Ex can also directly bind and inhibit Yki, restricting it to the cytoplasm. Regulators of Fat and Ds activity include: the Golgi-localized kinase Four-jointed (Fj); the cytoplasmic kinase Discs overgrown (Dco); and the cytoplasmic protein Lowfat (Lft). The transmembrane apical determinant Crumbs (Crb) interacts with Ex and, like Fat, is important for apical localization of Ex. The basolateral determinant Lgl can modulate Hpo activation. The Drosophila Ras association domain family protein, dRASSF, inhibits Hpo by competing with Sav for a binding site. In addition, the Drosophila LIM protein Ajuba (Jub) interacts with both Sav and Wts, inhibiting Yki phosphorylation (Badouel and McNeill, 2011; figure fromHalder and Johnson, 2011).

B) A normal (left) and yki-overexpressing (right) *Drosophila* wing imaginal disc (from Pan, 2010).

FIGURE 3

A

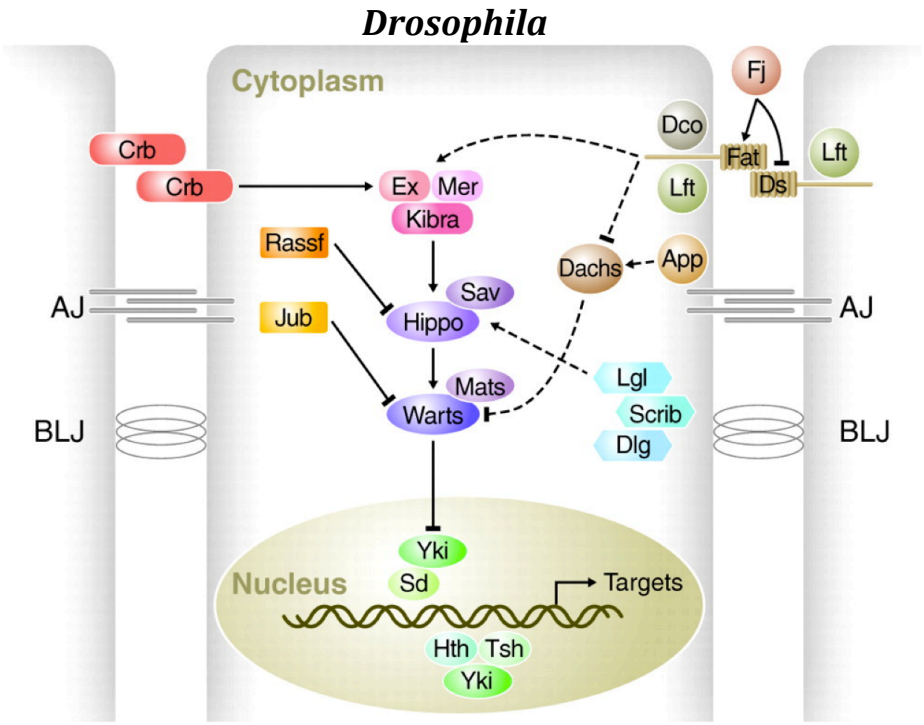
Drosophila
Cytoplasm
Fj
Dco
Fat
Lft
Ds
Crb
Crb
Ex
Mer
Kibra
Lft
Rassf
Dachs
App
Sav
AJ
Jub
Hippo
AJ
Mats
Lgl
Warts
Scrib
BLJ
Dlg
BLJ
Yki
Nucleus
Sd
Targets
Hth
Tsh
Yki

B

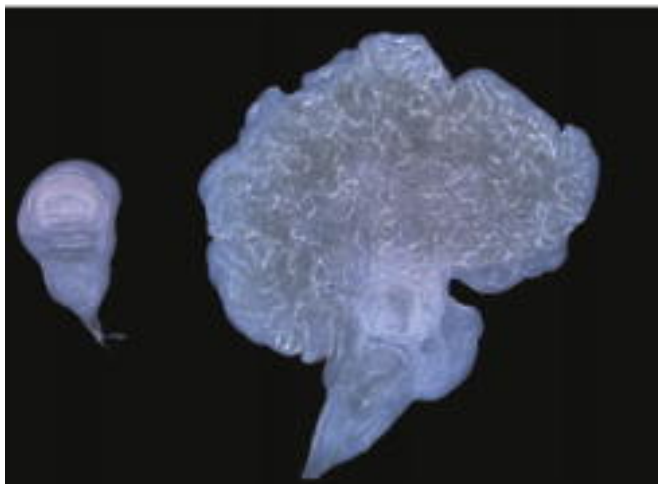

Figura 4. The Hippo signaling pathway in mammals

A) Signaling diagram of Hippo pathway in mammals. Similar to the invertebrate cascade, a series of phosphorylation events via MST and LATS ultimately leads to the phosphorylation of two Yki homologs: YAP and TAZ. In addition to cytoplasmic retention by 14-3-3, YAP/TAZ phosphorylation by the kinases LATS and CK1 leads to βTRCP-dependent proteasomal degradation of YAP/TAZ.
In the nucleus, both YAP and TAZ can bind to the Sd homologs TEAD1/4 and activate the transcription of genes required to promote cell growth and inhibit apoptosis. Another level of Hpo regulation occurs through CD44, MER, KIBRA, RASSF, AJUB, and the actin cytoskeleton. Their roles in mammals appear similar to their Drosophila orthologs, with the exception of RASSF, which is described as an MST activator. (Badouel and McNeill, 2011; figure from Halder and Johnson).

B) A normal (left) and a YAP-overepressing (right) mouse liver (from Pan, 2010).

FIGURE 4

A

Mammals

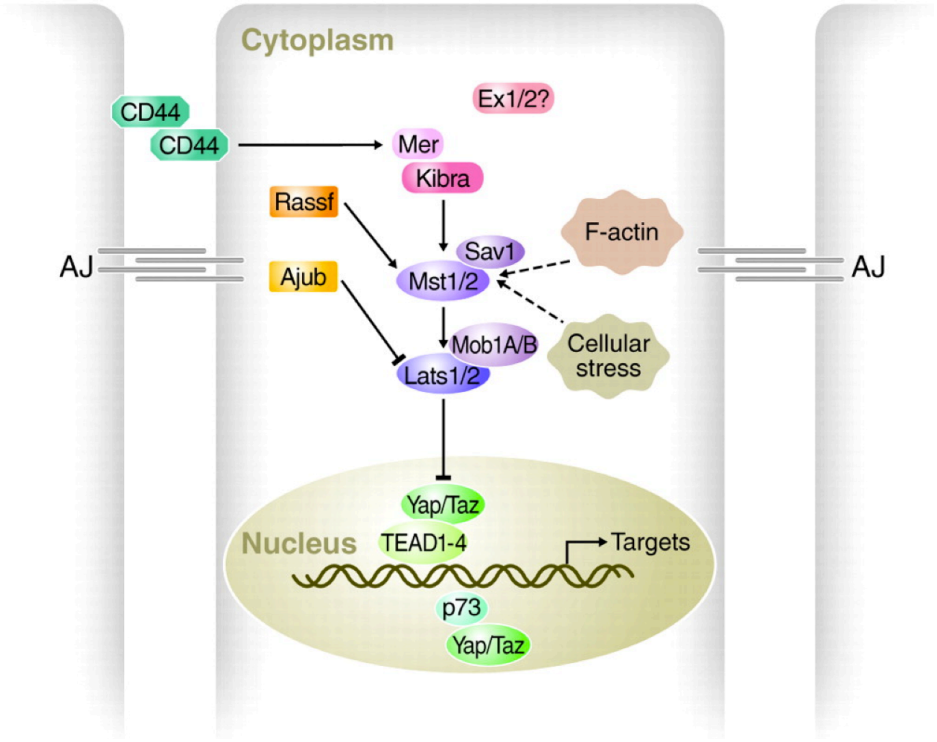

B

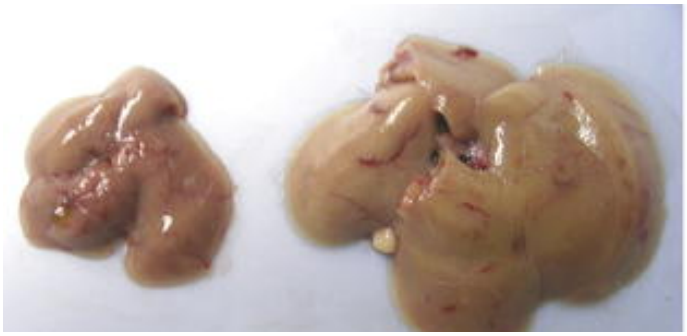

Figure 5. YAP/TAZ are regulated by ECM stiffness

A) Over-representation of YAP/TAZ target genes among the genes regulated by substrate stiffness in NMuMG mouse Mammary Epithelial Cells (MEC). Over-representation analysis was performed using one-sided Fisher's exact test (p-value<0.05). p- values were adjusted for False Discovery Rate (FDR<5%) (see Methods). Gene-sets highlighting activation of specific signaling pathways were derived from previously defined gene-expression signatures (see Methods for Refs.). Genes of WNT and β-catenin signatures were not represented in the stiffness signature. In yellow: over-representation reaches statistical significance only for the YAP/TAZ signatures.

B) Real-time PCR analysis in MCF10A cells (*CTGF* and *ANKRD1*, colored bars) and luciferase reporter assay in MDA-MB-231 cells (4XGTIIC-lux, black bars) to measure YAP/TAZ transcriptional activity. Cells were transfected with the indicated siRNAs (siCo. is the control siRNA, siYZ1 and siYZ2 are two YAP/TAZ siRNAs, see Methods) and cultured on plastic, or plated on stiff (elastic modulus of 40 KPa) and soft (0.7 KPa) fibronectin-coated hydrogels. Data are normalized to lane 1. (n=4).

C) Confocal immunofluorescence (IF) images of YAP/TAZ (green) and nuclei (red, TOTO3) of NMuMG MEC plated on stiff (40KPa) and soft (0.7KPa) fibronectin-coated acrylamide hydrogels. White bars = 15μm. Graphs on the right indicate the ratio of cells with nuclear YAP/TAZ; data are mean and SD (n=3; $^{**}P<0.01$).

D) Confocal immunofluorescence (IF) images of YAP/TAZ (green)and nuclei (red, TOTO3) in human Mesenchymal Stem Cells (hMSC) plated on stiff (40KPa) and soft (0.7KPa) fibronectin-coated acrylamide hydrogels. White bars = 15μm. Graphs on the right indicate the percentage of cells with nuclear YAP/TAZ. (n=3); data are mean and SD (n=3; $^{**}P<0.01$). Experiments were repeated n times with duplicate biological replicates.

FIGURE 5

A

signaling pathway	p-value
TGF-beta[a]	0.997
TGF-beta[b]	0.286
Ras	0.170
ERBB2	0.551
YAP/TAZ	**< 10^{-5}**
YAP	**< 10^{-5}**
Wnt	not represented
beta-catenin	not represented
Notch	0.997
NICD	0.997
NF-kappaB	0.997
MAL/SRF[a]	0.086
MAL/SRF[b]	0.125

B

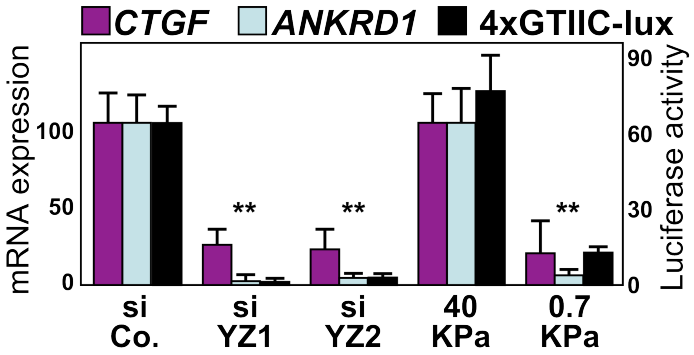

C

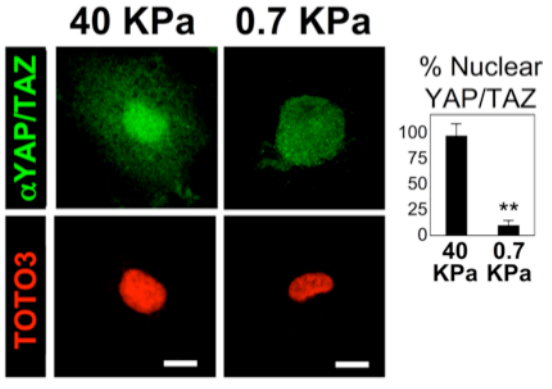

D

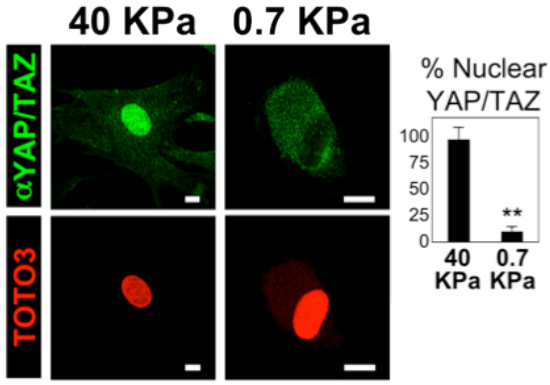

Figure 6. YAP/TAZ are regulated by cell shape

A) On top: gray patterns show the relative size of microprinted fibronectin islands on which cells were plated. Outline of a cell is shown superimposed to the leftmost unpatterned area (unpatt.). Below: Confocal IF images of YAP/TAZ (green) and nuclei (TOTO3, red) of hMSC plated on fibronectin islands of decreasing sizes (μm^2). White bars = 15μm. Graph provides quantifications. (n=8).

B) Constraining cell shape regulates YAP/TAZ nuclear localization also in Human Microvascular Endothelial Cells (HMVEC). Confocal IF images of endogenous YAP/TAZ (red) and actin filaments (phalloidin, green) in HMVEC plated on microprinted fibronectin islands of decreasing size (μm_2). White bars = 15μm. Right graphs provide complete quantifications. Data are mean and SD (n=7; **P*<0.05, ***P*<0.01).

C) On top: gray dots exemplify the distribution of fibronectin on micropillar arrays, shown superimposed with the outline of a cell. Below: representative IF of YAP/TAZ in hMSC plated on micropillars. White bars = 15μm. Graphs on the right: quantification of the projected cell area, total ECM contact area, and nuclear YAP/TAZ in hMSC plated on unpatterned fibronectin (unpatt.), micropillars and 300 μm2 islands. (n=4). All error bars are SD (*P<0.05; **P<0.01; Student's t-test is used throughout). Experiments were repeated n times with duplicate biological replicates.

D) Confocal IF images of hMSC plated on substrate of different stiffness (40 and 0.7 KPa) and stained for F-actin (Phalloidin) and nuclei (TOTO3). White bars = 15 μm.

FIGURE 6

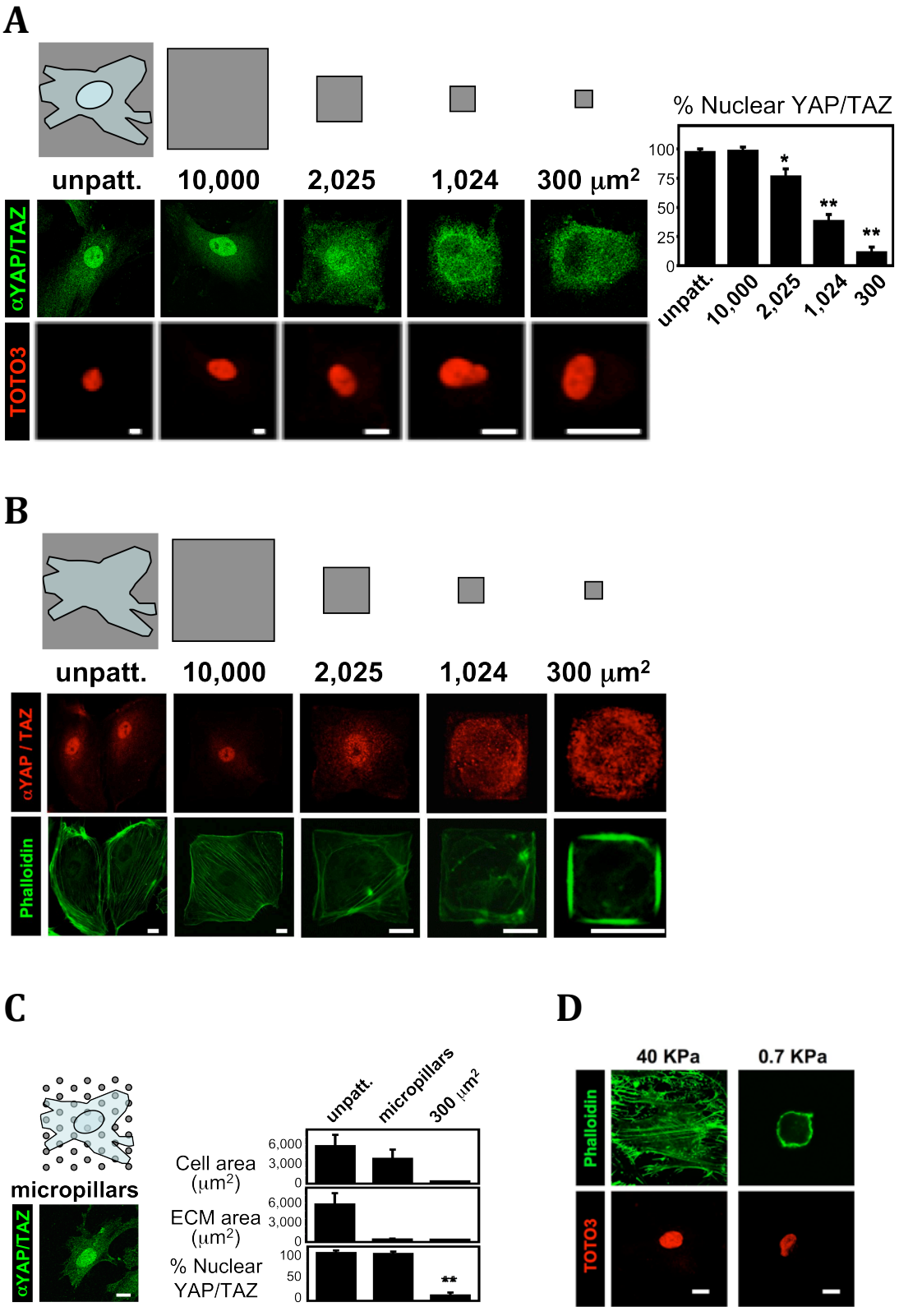
A
unpatt.
10,000
2,025
1,024
300 μm²
αYAP/TAZ
TOTO3
% Nuclear YAP/TAZ
100
75
50
25
0
*
**
**
unpatt.
10,000
2,025
1,024
300
B
unpatt.
10,000
2,025
1,024
300 μm²
αYAP / TAZ
Phalloidin
C
micropillars
αYAP/TAZ
unpatt.
micropillars
300 μm²
Cell area (μm²)
ECM area (μm²)
% Nuclear YAP/TAZ
6,000
3,000
0
6,000
3,000
0
100
50
0
**
D
40 KPa
0.7 KPa
Phalloidin
TOTO3

Figure 7. YAP/TAZ activity requires Rho and tension of the actin cytoskeleton

A) Confocal IF images of YAP/TAZ in hMSC treated with the Rho inhibitor C3 (3 μg/ml), the F-actin inhibitor LatrunculinA (Lat.A, 0.5μM), the Rac1-GEFs inhibitor NSC23766 (100μM) or the microtubule inhibitor Nocodazole (Noco. 30μM). White bars = 15μm. Graph provides quantifications (n=10).

B) Real-time PCR of MCF10A treated with cytoskeletal inhibitors as in (A). Data are normalized to untreated cells (Co.) (n=4).

C) Luciferase assay for YAP/TAZ activity in HeLa cells transfected with the indicated expression plasmids (Co. is empty vector, actin R62D encodes for a mutant unable to polymerize into F-actin) and treated with LatrunculinA. (n=4).

D) LEFT: Overexpression of activated Diaphanous (mDIA*) enhances YAP/TAZ transcriptional activity as assayed by luciferase activity in HeLa cells plated on plastics (Co.) or on soft ECM (1 KPa). Data are mean and SD (n=3; *P<0.05, **P<0.01). RIGHT, Upper panel: confocal IF images of HeLa cells transiently transfected with activated Diaphanous (FLAG-mDIA*). Transfected cells are stained with anti-FLAG (red channel). Staining with Phalloidin (green channel) shows enhanced stress-fibers in cells expressing active Diaphanous. Cells encircled by white dotted lines are non-transfected cells displaying background anti-FLAG staining and serve as internal controls. RIGHT, Lower panel: confocal IF images of HeLa cells transiently transfected with activated Diaphanous and mCherry as tracer (red channel) and stained for focal adhesions (Vinculin, green channel).

E) Overexpression of actin V159N and serum stimulation are unable to enhance YAP/TAZ. HeLa cells were transfected with 4xGTIIC-lux reporter together with empty vector (Co.), with activated Diaphanous (mDIA*), with a plasmid encoding for

V159N actin, or starved overnight without serum (- FCS) and subsequently treated with 20% serum (+ FCS). Data are mean and SD (n=5).

F) Positive controls for the activity of the R62D and V159N actin mutants.
LEFT: MAL/SRF-responsive element (SRF- lux) activity in HeLA cells treated as indicated and trasfected with R62D actin, using the same plasmid doses as in C. RIGHT: HeLa cells transfected with SRF-lux, showing effective enhancement of MAL/SRF activity upon expression of mDIA*, V159N actin and FCS (20% serum) stimulation. Plasmid doses used were the same as in E. Co. indicates transfection with empty vector. All data are mean and SD (n=5).
All error bars are SD (*P<0.05; **P<0.01). Experiments were repeated n times with duplicate biological replicates.

FIGURE 7

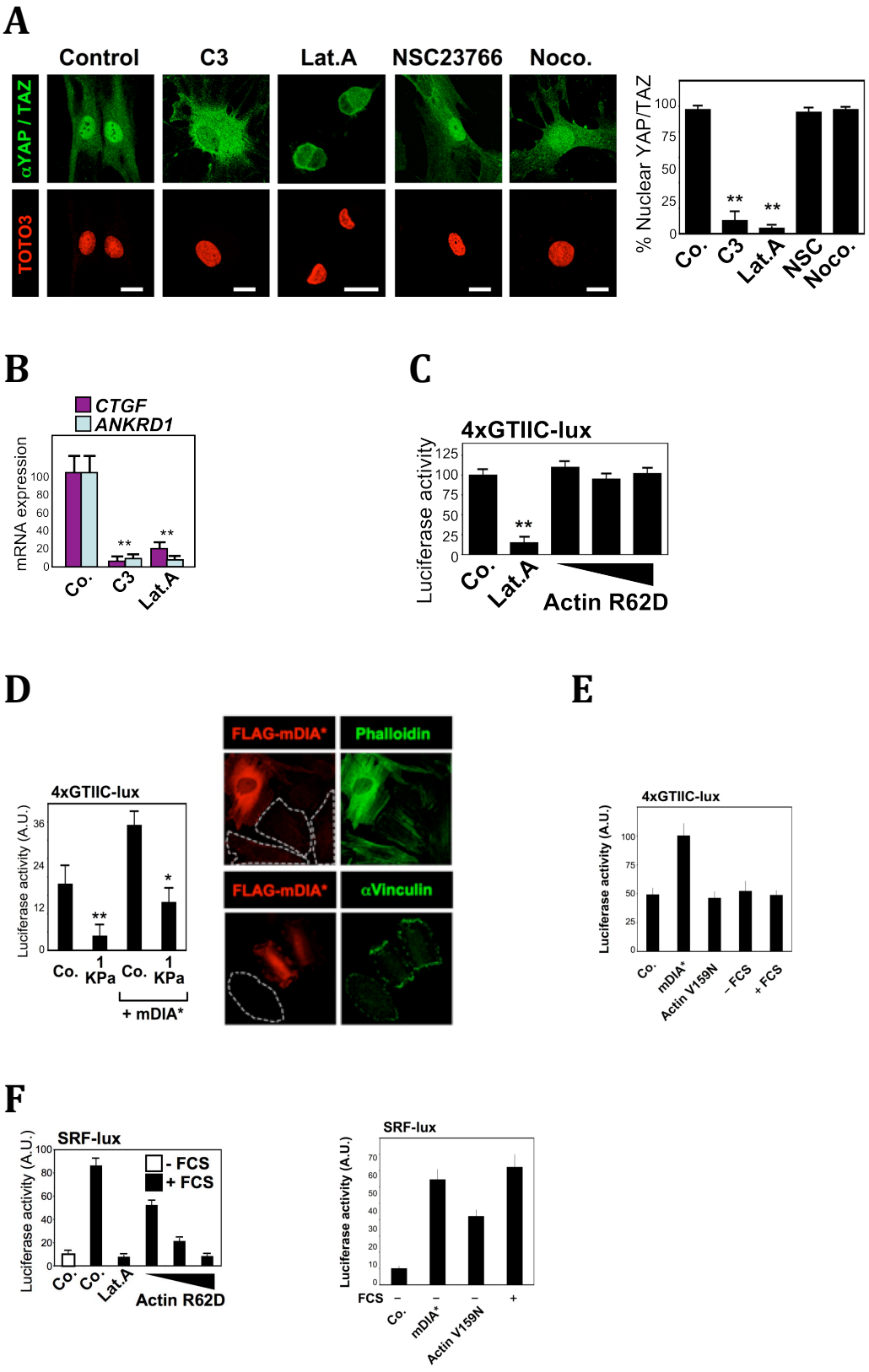
A
Control
C3
Lat.A
NSC23766
Noco.
αYAP / TAZ
TOTO3
% Nuclear YAP/TAZ
Co.
C3
Lat.A
NSC
Noco.
B
CTGF
ANKRD1
mRNA expression
Co.
C3
Lat.A
C
4xGTIIC-lux
Luciferase activity
Co.
Lat.A
Actin R62D
D
4xGTIIC-lux
Luciferase activity (A.U.)
Co.
1 KPa
Co.
1 KPa
+ mDIA*
FLAG-mDIA*
Phalloidin
FLAG-mDIA*
αVinculin
E
4xGTIIC-lux
Luciferase activity (A.U.)
Co.
mDIA*
Actin V159N
– FCS
+ FCS
F
SRF-lux
Luciferase activity (A.U.)
- FCS
+ FCS
Co.
Co.
Lat.A
Actin R62D
SRF-lux
Luciferase activity (A.U.)
FCS
Co.
mDIA*
Actin V159N

Figure 8. The relashionship between force and YAP/TAZ

A) Confocal IF images of hMSC treated with the ROCK inhibitor Y27632 (50mM), or the non-muscle myosin inhibitor Blebbistatin (Blebbist. 50mM). YAP/TAZ (green) and nuclei (red). White bars = 15mm. Graph provides quantifications (n=9).

B) Luciferase activity of the YAP/TAZ reporter in HeLa treated with the ROCK inhibitor Y27632 (50mM), or the non-muscle myosin inhibitor Blebbistatin (Blebbist. 50mM),as in (A).

C) Confocal IF images of hMSC cells plated on fibronectin-coated glass slides and treated for different periods (2 and 6 hours, respectively) with the indicated inhibitors of ROCK (Y27632) or non-muscle myosin (Blebbistatin). Cells were stained for YAP/TAZ (red channel), F-actin (Phalloidin, green channel) and nuclei (Hoechst, blue channel). Graphs provide the quantifications of nuclear YAP/TAZ. Data are mean and SD (n=3). Note how inhibition of cytoskeletal tension after 2 hours influences YAP/TAZ localization before affecting stress-fiber integrity.

D) Confocal IF images of hMSC plated on arrays of micropillars of different rigidities. On rigid micropillars (black lines) cells develop cytoskeletal tension (blue arrow) by pulling against the ECM (orange arrow); cells bend elastic micropillars and develop reduced tension exemplified by reduced size of the arrows. White bars = 15mm. Graph provides quantifications. (n=2). All error bars are SD (*P<0.05; **P<0.01). Experiments were repeated n times with duplicate biological replicates.

FIGURE 8

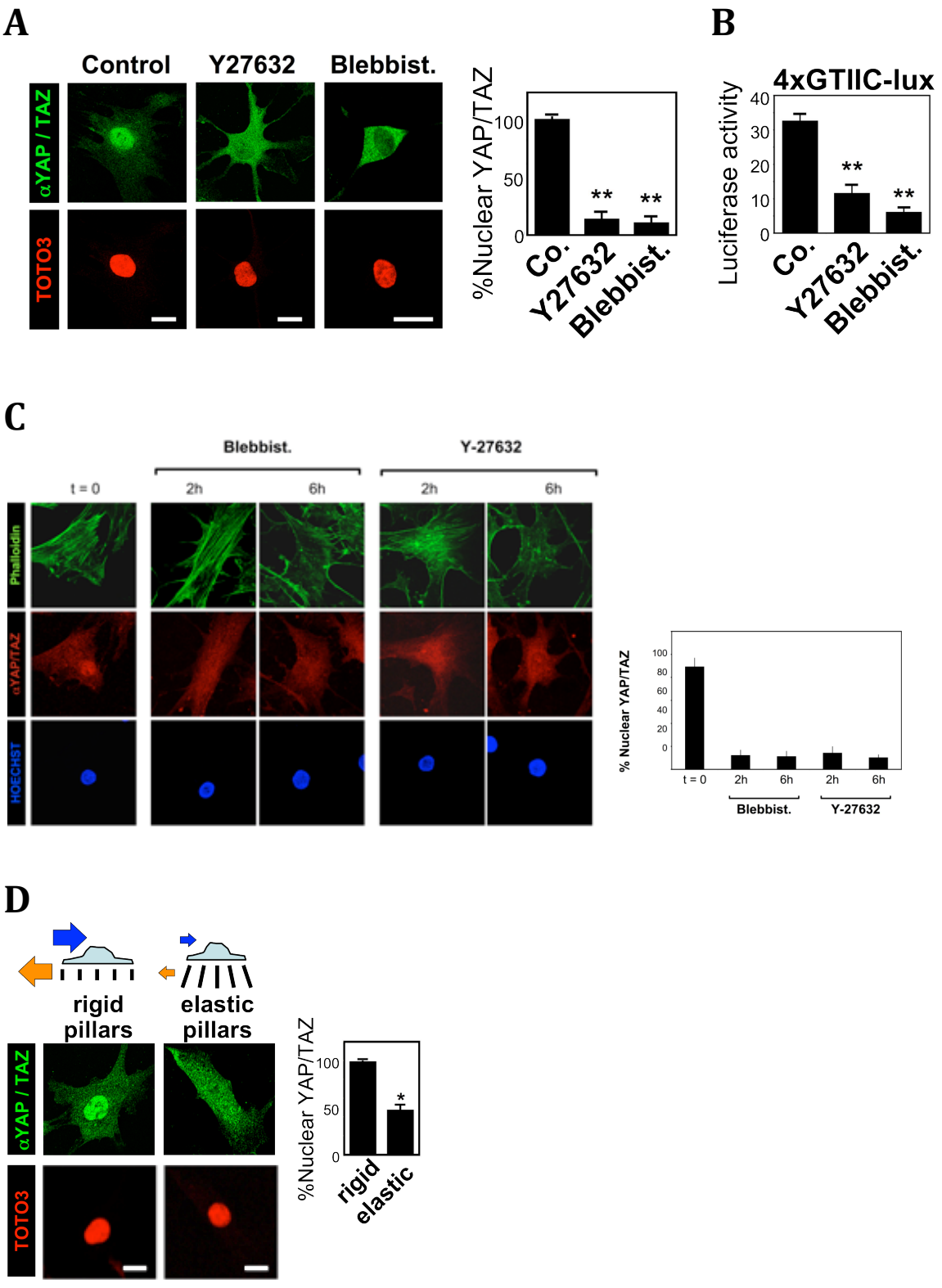
A
Control
Y27632
Blebbist.
αYAP / TAZ
TOTO3
%Nuclear YAP/TAZ
100
50
0
**
**
Co.
Y27632
Blebbist.
B
4xGTIIC-lux
Luciferase activity
40
30
20
10
0
**
**
Co.
Y27632
Blebbist.
C
Blebbist.
Y-27632
t = 0
2h
6h
2h
6h
Phalloidin
αYAP/TAZ
HOECHST
% Nuclear YAP/TAZ
100
80
60
40
20
0
t = 0
2h
6h
2h
6h
Blebbist.
Y-27632
D
rigid pillars
elastic pillars
αYAP / TAZ
TOTO3
%Nuclear YAP/TAZ
100
50
0
*
rigid
elastic

Figure 9. YAP/TAZ localization is regulated by cytoskeletal tension at the level of nuclear retention

A) YAP/TAZ confocal immunofluorescent microscopy of hMSC plated on fibronectin-coated slides and treated with the ROCK inhibitor Y27632 to exclude YAP/TAZ from nuclei (t=0) and then also treated with the inhibitor of CRM1-dependent nuclear export Leptomycin B (LMB, 40ng/ml) for 2 additional hours. Quantifications are shown as mean and SD (n=3). LMB treatment restores YAP/TAZ nuclear localization in cells with relaxed acto- myosin cytoskeleton. White bars = 15μm.

B) Confocal IF pictures of hMSC that were plated on fibronectin- coated glass, and treated with the indicated small molecule inhibitors to cause YAP/TAZ exclusion (t=0). Y27632 is a ROCK inhibitor; LatrunculinA (Lat.A) is an F-actin inhibitor. Inhibitors were then removed (washout) and cells were incubated in normal medium for 4 more hours before fixation. White bars = 15 μm.

C) Cytoskeletal inhibition regulates YAP/TAZ localization independently of de novo protein synthesis. YAP/TAZ confocal IF of hMSC, treated with cycloheximide (CHX, 0,25mg/ml) to block protein synthesis, and then subsequently treated for 1 hour also in the presence of LatrunculinA (Lat.A). White bars = 15mm.

FIGURE 9

A

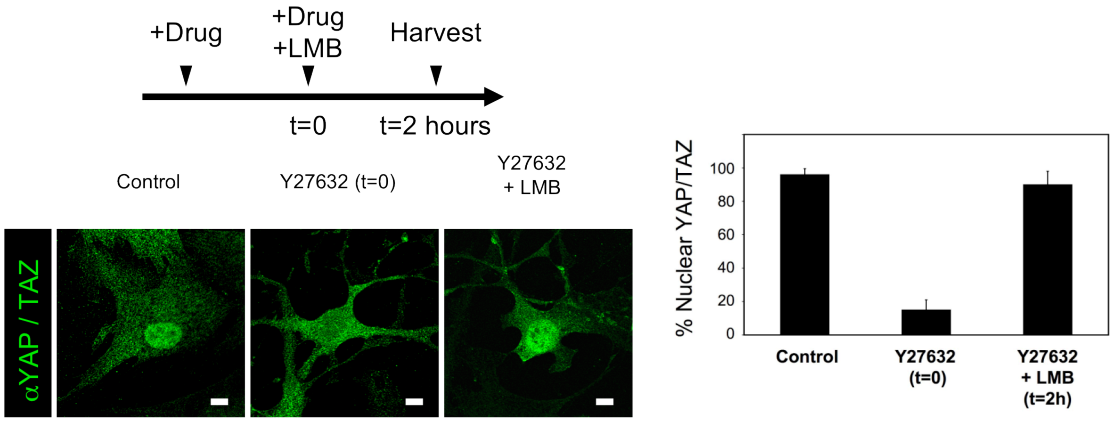
+Drug
+Drug
+LMB
Harvest
t=0
t=2 hours
Control
Y27632 (t=0)
Y27632
+ LMB
αYAP / TAZ
% Nuclear YAP/TAZ
100
80
60
40
20
0
Control
Y27632
(t=0)
Y27632
+ LMB
(t=2h)

B

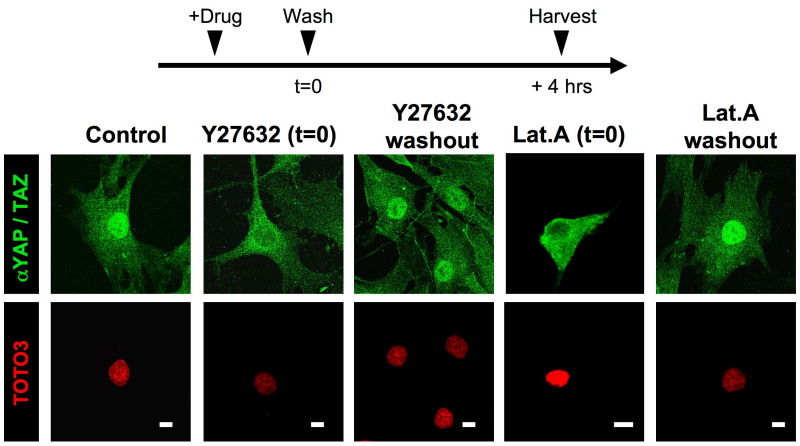
+Drug
Wash
Harvest
t=0
+ 4 hrs
Control
Y27632 (t=0)
Y27632
washout
Lat.A (t=0)
Lat.A
washout
αYAP / TAZ
TOTO3

C

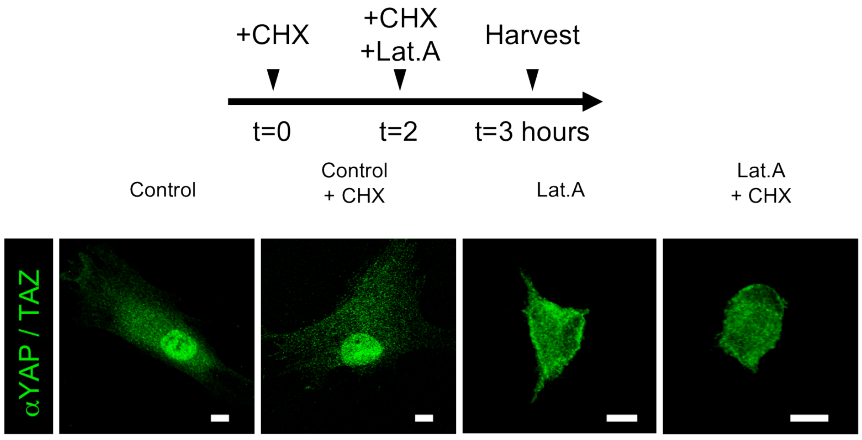
+CHX
+CHX
+Lat.A
Harvest
t=0
t=2
t=3 hours
Control
Control
+ CHX
Lat.A
Lat.A
+ CHX
αYAP / TAZ

Figure 10. ECM stiffness and cell spreading regulate YAP/TAZ independently of the Hippo pathway

A) Immunoblotting for the indicated proteins in MCF10A plated on plastic at low (sparse) or high (dense) confluence and plated on stiff (40 KPa) or soft (0.7 KPa) hydrogels.

B) Immunoblotting for the indicated proteins in MCF10A treated with C3 and LatrunculinA (Lat.A) compared to untreated cells (Co.) P-S127 is phospho-YAP.

C) Quantification of nuclear YAP/TAZ in hMSC transfected with control- or LATS1/2-siRNA #A and plated on microprinted islands of different size (n=4).

D) Immunoblotting from hMSC cells transfected with the indicated siRNAs (Co.=control siRNA, L=LATS1/2 siRNA #A), plated on plastic and treated with C3 (0.5 or 3 mg/ml).

E) Real-time PCR analysis of MCF10A transfected with the indicated siRNAs and cultured on hydrogels. Data are normalized to the first lane (n=3).

F) Luciferase assay in MDA-MB-231 transfected as indicated and treated with LatrunculinA (Lat.A) or replated on soft hydrogels. (n=8).

G) RT-PCR of MCF10A cultured under sparse or confluent (dense) conditions on the indicated hydrogels. Data are normalized to the first lane (n=2). All error bars are SD (*P<0.05; **P<0.01). Experiments were repeated n times with duplicate biological replicates.

FIGURE 10

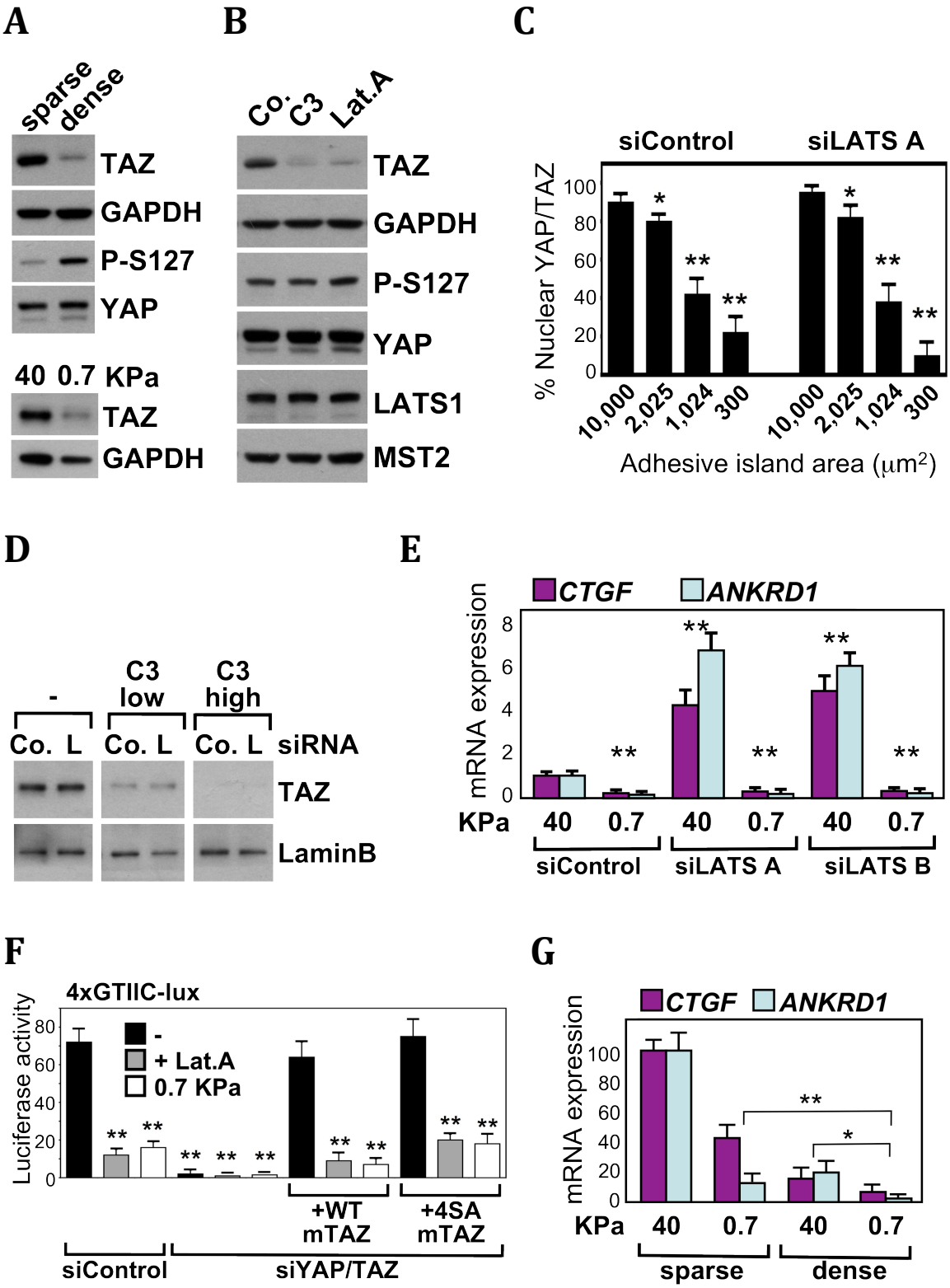
A
sparse
dense
TAZ
GAPDH
P-S127
YAP
40 0.7 KPa
TAZ
GAPDH
B
Co.
C3
Lat.A
TAZ
GAPDH
P-S127
YAP
LATS1
MST2
C
siControl
siLATS A
% Nuclear YAP/TAZ
100
80
60
40
20
0
*
**
**
**
*
**
**
10,000
2,025
1,024
300
10,000
2,025
1,024
300
Adhesive island area (μm2)
D
-
C3 low
C3 high
Co. L
Co. L
Co. L
siRNA
TAZ
LaminB
E
CTGF
ANKRD1
mRNA expression
8
6
4
2
0
**
**
**
**
**
**
KPa
40
0.7
40
0.7
40
0.7
siControl
siLATS A
siLATS B
F
4xGTIIC-lux
Luciferase activity
80
60
40
20
0
-
+ Lat.A
0.7 KPa
**
**
**
**
**
**
**
**
**
**
+WT mTAZ
+4SA mTAZ
siControl
siYAP/TAZ
G
CTGF
ANKRD1
mRNA expression
100
80
60
40
20
0
**
*
KPa
40
0.7
40
0.7
sparse
dense

Figure 11. YAP/TAZ mediates hMSC differentiation controlled by ECM elasticity

A) hMSC were transfected with the indicated siRNA (control, siCo.; YAP/TAZ, siYZ1 and siYZ2), plated on stiff (40 KPa) or soft (1 KPa) substrates and induced to differentiate into osteoblasts. C3 (0.5μg/ml) was added and renewed with differentiation medium. Representative alkaline phosphatase stainings and (b) quantifications of osteogenic differentiation. (n=4); (c) quantification of adipogenesis based on oil-red stainings. (n=2) (A.U., arbitrary units, see methods).

B) Quantifications of osteogenic differentiation (n=4) of cells treated as in A. (A.U., arbitrary units, see methods).

C) hMSC were transfected with the indicated siRNA (control, siCo.; YAP/TAZ, siYZ1 and siYZ2), plated on stiff (40 KPa) or soft (1 KPa) substrates and induced to differentiate into adipocytes. C3 (0.5mg/ml) was added and renewed with differentiation medium. LEFT: Top row: low magnification pictures of representative oil-red stainings of hMSC Hoechst staining shows nuclei of the same cells of the oil-red pictures above. Bottom row: close-up of representative differentiated hMSC. Note how the differences in adipogenic differentiation between samples were not only quantitative (i.e. number of cells displaying oil-red staining) but also qualitative (i.e. amount of vacuoles per cells).
RIGHT: quantification of adipogenesis differentiation (n=2) (A.U., arbitrary units, see methods). Experiments were repeated n times, $^{**}P<0.01$.

FIGURE 11

A

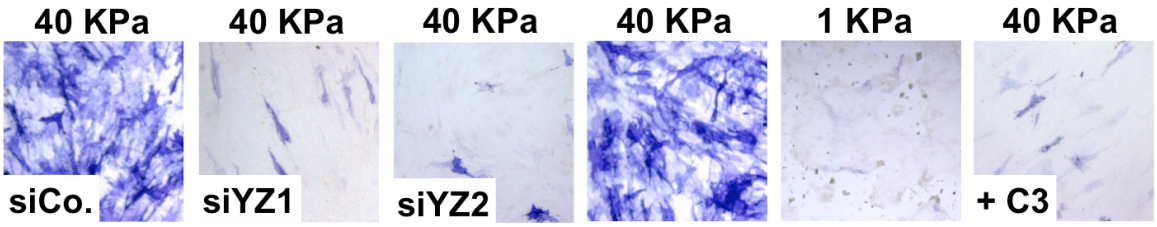

B

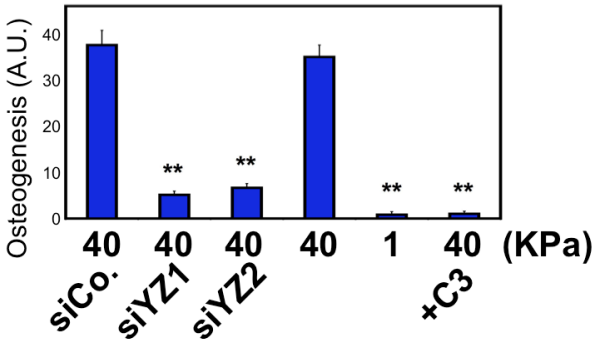

C

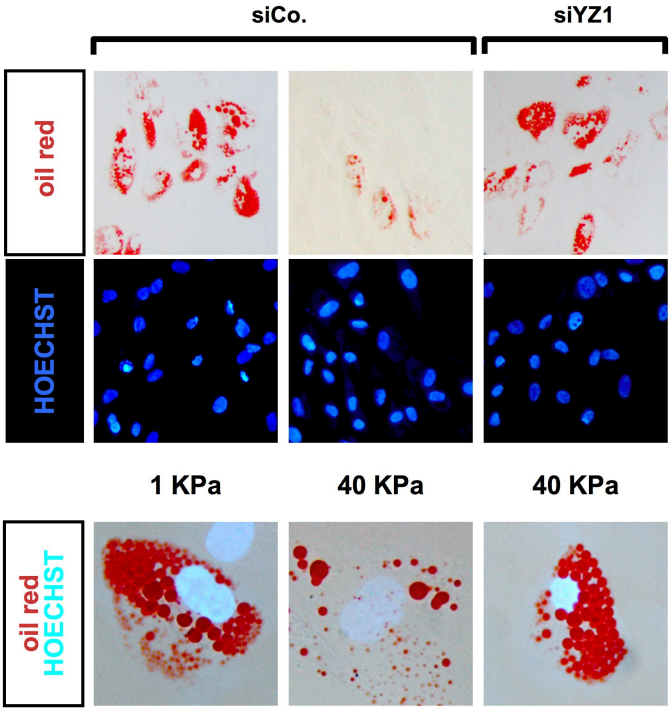

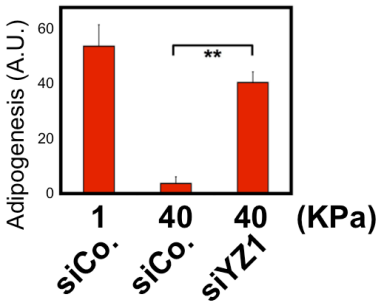

Figure 12. YAP/TAZ are required mediators of the biological effects controlled by cell geometry

A) Representative BrdU stainings of HMVEC plated on adhesive islands of different size; where indicated, cells were treated o.n. with C3 (2.5mg/ml), or transfected with the indicated siRNAs. (n=5). Hoechst staining (in blue) shows nuclei of the corresponding fields. Gray squares on top show the relative dimensions of the single patterns where cells were seeded on; the black bar at the bottom right serves as scale bar for the pictures.

B) Representative TUNEL stainings of HMVEC plated on adhesive islands of different size; where indicated, cells were treated o.n. with C3 (2.5mg/ml), or transfected with the indicated siRNAs. (n=5). Hoechst staining (in blue) shows nuclei of the corresponding fields. Gray squares on top show the relative dimensions of the single patterns where cells were seeded on; the black bar at the bottom right serves as scale bar for the pictures.

C) Quantifications of proliferation of HMVEC transfected with the indicated siRNAs and plated on adhesive islands of different sizes, indicated below each column (μm^2). All data are mean and SD (n=3).

D) Proliferation (upper panel) and apoptosis (lower panel) of control and 5SA-YAP-expressing HMVEC, plated on adhesive islands. Experiments were repeated n times with duplicate biological replicates, $^{**}P<0.01$.

FIGURE 12

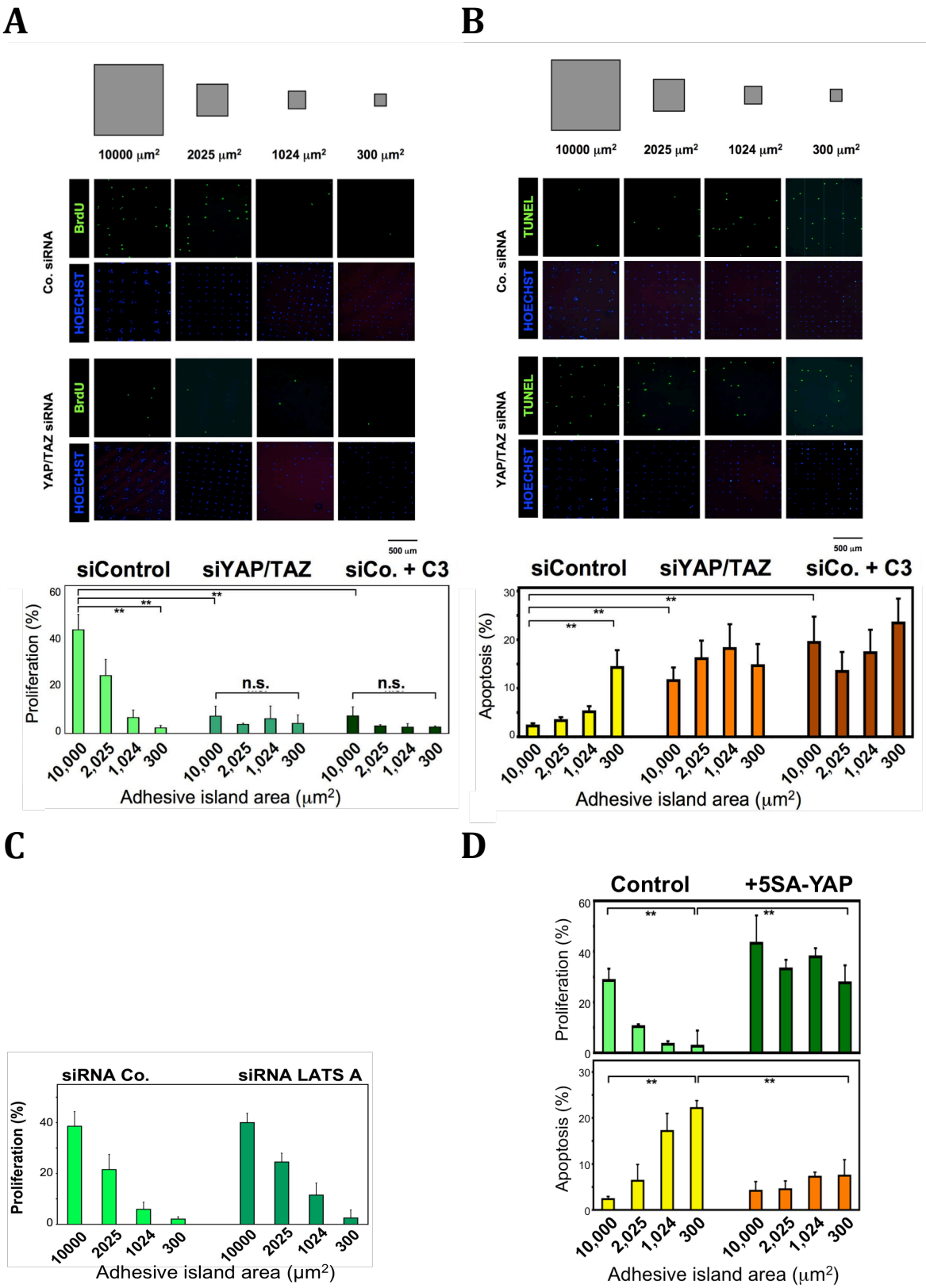
A
B
10000 μm²
2025 μm²
1024 μm²
300 μm²
Co. siRNA
YAP/TAZ siRNA
BrdU
TUNEL
HOECHST
500 μm
siControl
siYAP/TAZ
siCo. + C3
Proliferation (%)
Apoptosis (%)
n.s.
10,000
2,025
1,024
300
Adhesive island area (μm²)
C
D
siRNA Co.
siRNA LATS A
Control
+5SA-YAP

Figure 13. Cells respond to their physical microenvironment according to YAP/TAZ activity

A) Representative alkaline phosphatase stainings and quantification of osteogenesis in hMSC transduced with 5SA-YAP, and treateted with C3 (50 and 150 ng/ml) (n=3).

B) Quantifications of osteogenic differentiation of control siRNA (siRNA Co.) and LATS siRNA (siRNA LATS A) transfected hMSC. Cells were transfected, replated, and induced to differentiate in the absence (-) or in the presence of increasing doses of the Rho inhibitor C3 (+C3; low dose = 50ng/ml, high dose = 150ng/ml).

C) Quantifications of osteogenesis in hMSC transduced with 5SA-YAP and plated on hydrogels (n=2). All error bars are SD (*P<0.05; **P<0.01; n.s. not significant). Experiments were repeated n times with duplicate biological replicates.

FIGURE 13

A

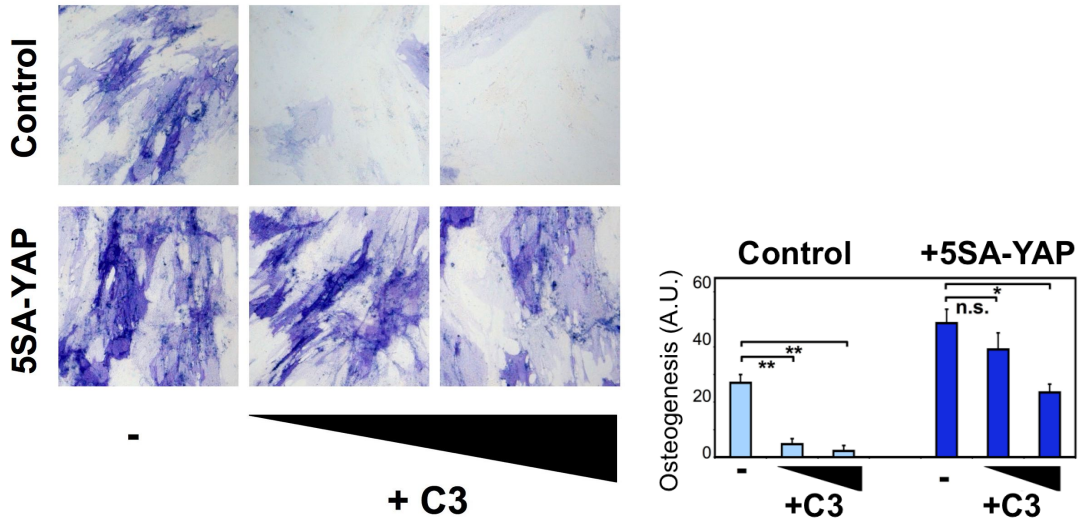

B

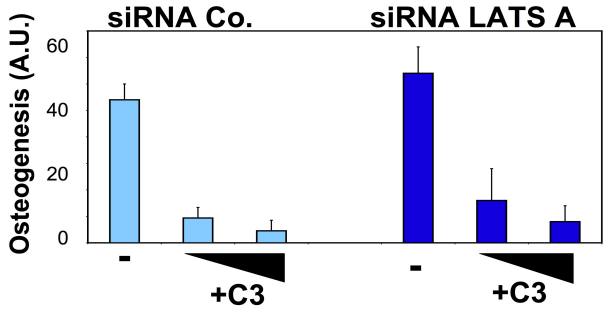

C

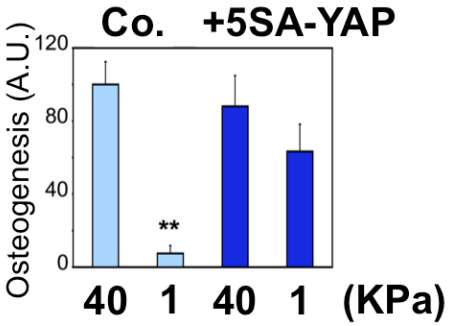

Figure 14. Role of YAP/TAZ in mechanotransduction

A) A model for the role of YAP/TAZ as readers and effectors of cell behavior induced by the mechanical/physical properties of the cellular microenvironment, such as ECM stiffness, cell spreading and cytoskeletal tension. On the left: Cells growing on stiff substrates (indicated in grey) can develop cytoskeletal tension by pulling on the ECM, which permits the maturation of cell-substrate adhesions3 (indicated by the symbol ||) and the development of stress-fibers (indicated by the black lines in the cytoplasm). In these conditions, YAP/TAZ transcriptional coactivators (indicated in green) accumulate in the nucleus and can regulate gene transcription, enabling cells to behave according to the mechanical microenvironment. On the right: Cells growing on soft substrates (indicated in pink) cannot develop cytoskeletal tension and display reduced or no stress-fibers (black lines abutting the cell membrane indicate the formation of the cortical F-actin cytoskeleton). In these conditions, YAP/TAZ are excluded from the nucleus and accumulate in the cytoplasm (now stained in green). In this case, it is the absence of YAP/TAZ transcriptional activity that instructs cell behavior in response to the microenvironment.

B) A model of YAP/TAZ regulatin by the canonical Hippo pathway and by mechanical/physical properties of the cellular microenvironment. Pointed and blunt arrowheads indicate activating or inhibitory interactions, respectively. Known interactions are indicated by solid lines whereas dashed lines indicate supposed mechanisms. Blue arrowheads indicate feedbacks.

FIGURE 14

A

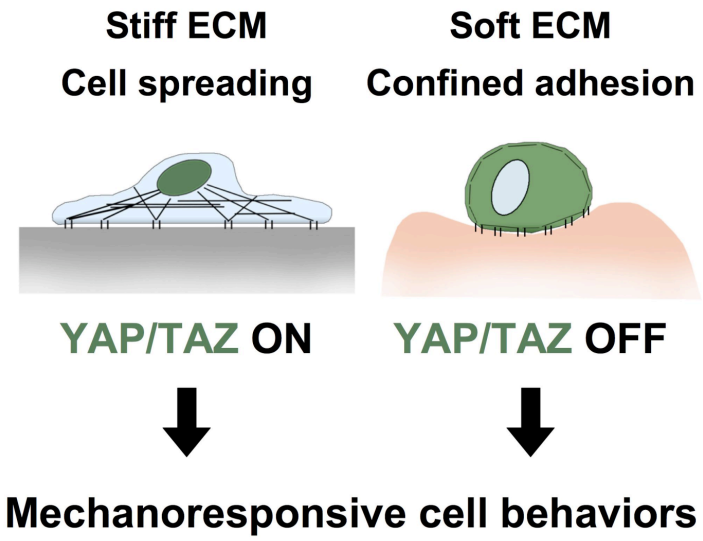
Stiff ECM
Cell spreading
Soft ECM
Confined adhesion
YAP/TAZ ON
YAP/TAZ OFF
Mechanoresponsive cell behaviors

B

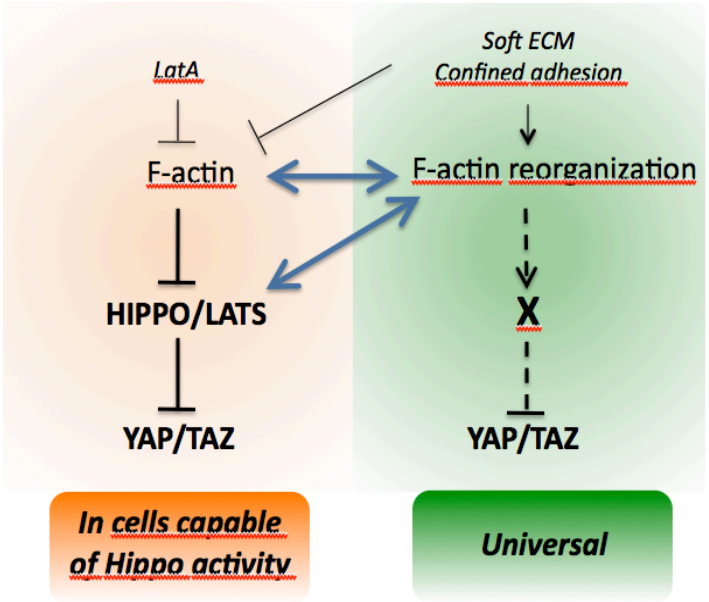
LatA
Soft ECM
Confined adhesion
F-actin
F-actin reorganization
HIPPO/LATS
X
YAP/TAZ
YAP/TAZ
In cells capable of Hippo activity
Universal